Discovery of novel TNNI3K inhibitor suppresses pyroptosis and apoptosis in murine myocardial infarction injury

Haiying Pang, Ning Wang, Jinlong Chai, Xiaoyun Wang, Yuehua Zhang, Zhiang Bi, Wenbin Wu, Gu He

PII: S0223-5234(20)30283-X

DOI: https://doi.org/10.1016/j.ejmech.2020.112314

Reference: EJMECH 112314

To appear in: *European Journal of Medicinal Chemistry*

Received Date: 27 February 2020

Revised Date: 6 April 2020

Accepted Date: 6 April 2020

Please cite this article as: H. Pang, N. Wang, J. Chai, X. Wang, Y. Zhang, Z. Bi, W. Wu, G. He, Discovery of novel TNNI3K inhibitor suppresses pyroptosis and apoptosis in murine myocardial infarction injury, *European Journal of Medicinal Chemistry* (2020), doi: https://doi.org/10.1016/j.ejmech.2020.112314.

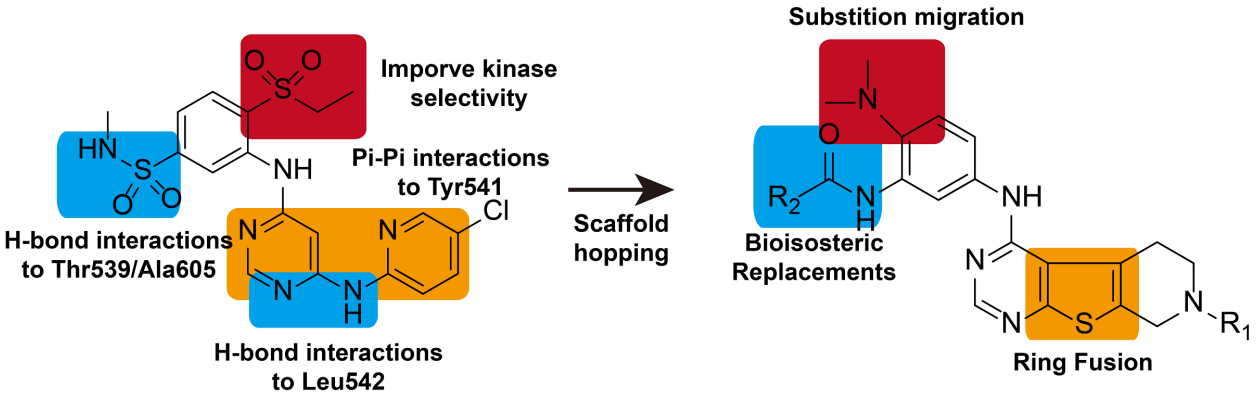

Discovery of novel TNNI3K inhibitor suppresses pyroptosis and apoptosis in murine myocardial infarction injury

Haiying Pang,[1,†] Ning Wang,[1,†] Jinlong Chai,[1] Xiaoyun Wang,[1] Yuehua Zhang,[1] Zhiang Bi,[1] Wenbin Wu,[2] and Gu He[1,*]

1 State Key Laboratory of Biotherapy and Cancer Center, West China Hospital, Sichuan University and Collaborative Innovation Center, Chengdu, Sichuan 610041, PR China

2 Department of Neurology, Chongzhou People's Hospital, Chengdu 611230, China

† These authors contributed equally to this work.

Abstract

Myocardial infarction (MI) injury is a highly lethal syndrome that has, until recently, suffered from a lack of clinically efficient targeted therapeutics. The cardiac troponin I interacting kinase (TNNI3K) exacerbates ischemia-reperfusion (IR) injury via oxidative stress, thereby promoting cardiomyocyte death. In this current study, we designed and synthesized 35 novel TNNI3K inhibitors with a pyrido[4,5]thieno[2,3-d] pyrimidine scaffold. *In vitro* results indicated that some of the inhibitors exhibited sub-micromolar TNNI3K inhibitory capacity and good kinase selectivity, as well as cytoprotective activity, in an oxygen-glucose deprivation (OGD) injury cardiomyocyte model. Furthermore, investigation of the mechanism of the representative derivative compound 6o suggested it suppresses pyroptosis and apoptosis in cardiomyocytes by interfering with p38MAPK activation, which was further confirmed in a murine myocardial infarction injury model. *In vivo* results indicate that compound 6o can markedly reduce myocardial infarction size, decrease circulating cardiac troponin I (cTnI) leakage, and alleviate cardiac tissue damage in rats. In brief, our results provide the basis for further development of novel TNNI3K inhibitors for targeted MI therapy.

Keywords: TNNI3K inhibitor, Structure-activity relationships, Pyroptosis, Myocardial infarction

1. Introduction

Acute myocardial infarction (AMI), a type of myocardial necrosis associated with acute, persistent ischemia and hypoxia in coronary arteries, can cause various symptoms including arrhythmia, adverse remodeling, and systolic dysfunction. AMI remains a leading cause of morbidity and death worldwide.[1] Timely treatment using percutaneous coronary intervention (PCI), the preferred treatment of AMI, can minimize ischemic injury, limit MI size, and inhibit ventricular remodeling to protect heart function, and improve the survival rate of MI. However, at the same time, reperfusion injury caused by PCI promotes reactive oxygen species (ROS) generation, intracellular Ca^{2+} overload and upregulation of pro-inflammatory molecules, which leads to death of viable cardiomyocytes and cardiac dysfunction during ischemia.[2-4] Although a large number of studies on various drugs and methods for preventing myocardial cell death during myocardial ischemia and reperfusion have been published,[5-8] patients with myocardial ischemia/reperfusion injury still lack effective therapeutic drugs, especially novel cardio-protective and myocardial recovery agents, which makes research into this field particularly important.[9-14]

Cardiac troponin I interacting kinase (TNNI3K), a member of the mitogen-activated protein kinase kinase kinase (MAPKKK) family and the cardiac ankyrin repeat kinase (CARK), is selectively expressed in heart tissue and is observed in fetal and adult hearts. TNNI3K is almost non-existent in all other tissues except for trace expression in the brain and testes.[15-19] In humans, the longest TNNI3K isoform encodes a 92 kD protein composed of 835 amino acids that contain three

types of recognizable domains: 10 N-terminal ankyrin repeats, a central kinase domain and a C-terminal Ser-rich domain.[15] TNNI3K overexpression and knockout mouse models indicate that TNNI3K can increase infarct size in ischemic hearts, induce mitochondrial ROS generation, cause mitochondrial dysfunction and bioenergy damage in cardiomyocytes. TNNI3K is also associated with activation of p38 mitogen-activated protein kinase MAPK to exacerbate ischemic injury and myocardial cell death.[16, 20] Research indicates that TNNI3K likely plays a crucial role in significant parts of cardiac biology and cardiac diseases including supraventricular tachycardia, viral myocarditis, cardiac conduction, cardiomyopathy, obesity and metabolic disease, as well as pathological and physiological hypertrophy,[21-23] suggesting that TNNI3K is a promising treatment target for cardiac disease.

Although TNNI3K is a potential therapeutic target for heart disease, there have only been a few reports of feasibility studies of TNNI3K inhibitors as potential agents. All preclinical study results were reported by Brian G. Lawhorn *et al.* In 2015, 7-deazapurine derivatives was first reported as dual TNNI3K/B-Raf inhibitors. As B-raf kinase inhibition has been linked to effects in heart failure models, 7-deazapurine compounds did not fully characterize the function of TNNI3K in cardiac biology.[24] Subsequently, GSK114, which developed based on 7-deazapurine, displayed excellent cellular activity (IC_{50}=25nM) and showed appreciable selectivity over B-Raf (>40 fold).[25] GSK854 was first reported in 2018 as a highly selective TNNI3K inhibitor (IC_{50}=25nM),[26] but the 4,6-diaminopyrimidine structure of GSK854 has been proven to be clinically relevant and an extensively explored structural class of kinase inhibitors, such as EGFR.[24-26]

GSK114 and GSK854 serve as useful TNNI3K inhibitors for cellular and *in vivo* models and are available as probes, which can help elucidate the biological pathways that are associated with TNNI3K in heart disease (Figure 1A). However, there is no clinical data from GSK114 and GSK854.[24-27] We attempted to develop a novel and sufficiently selective TNNI3K inhibitor based on the interaction between GSK854 and the known crystal structure of TNNI3K by means of framework transitions, ring fusion and other mechanisms (Figure 1B).

In this current study, we reported the rationale, the design, chemical synthesis, and *in vitro* and *in vivo* evaluation of pyrido[4,5] thieno[2,3-d] pyrimidine-based TNNI3K inhibitors as a potential lead compound against AMI. *In vitro* kinase inhibition and selectivity assays, cell proliferation and programmed cell death assays were measured, alongside the molecular mechanisms of these novel TNNI3K inhibitors. These results suggested that the novel TNNI3K inhibitors pyrido[4,5]thieno[2,3-d] pyrimidine derivatives efficiently suppressed ROS accumulation, apoptotic and pyroptotic cell death in oxygen and glucose deprivation (OGD) H9c2 cells via a p38-MAPK signaling pathway. Furthermore, pyrido[4,5]thieno[2,3-d] pyrimidine derivatives significantly reduced cardiomyocyte apoptosis, pyroptosis and tissue fibrosis in a rat myocardial ischemia/reperfusion model without obvious morphological changes in the main organs, which suggests that these TNNI3K inhibitors are worth further development.

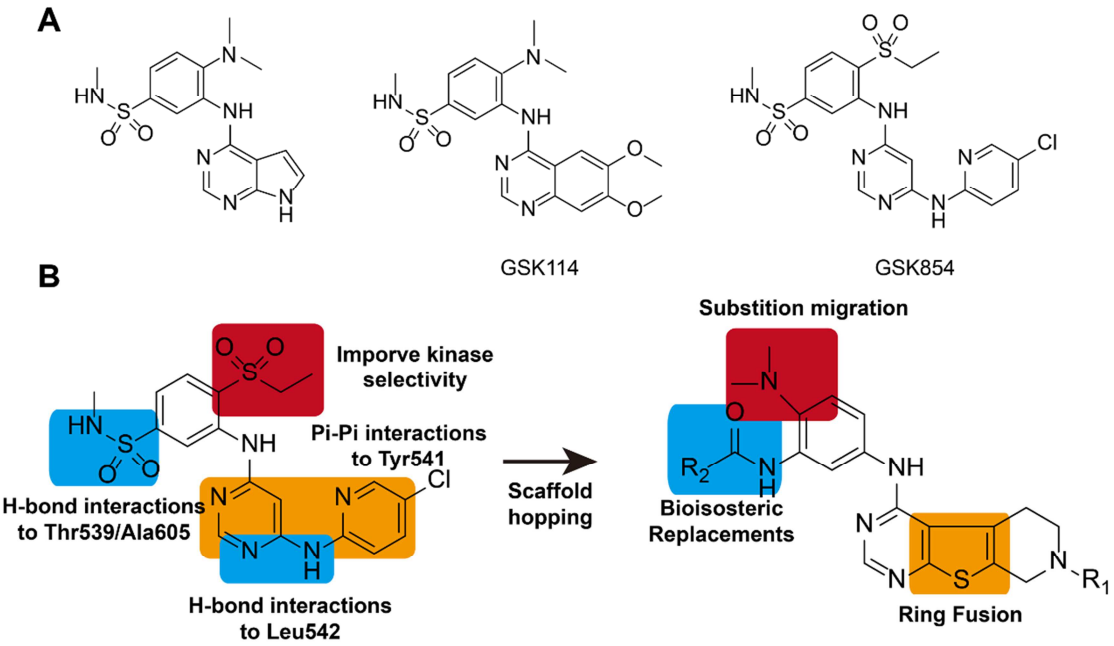

Figure 1. (A) Chemical structures of representative TNNI3K inhibitors; (B) The scaffold hoping strategy of novel TNNI3K inhibitors.

2. Results and Discussion

2.1 Chemistry

The synthesis of target compounds is depicted on Scheme 1. A series of differently substituted N-(5-amino-2-(dimethylamino) phenyl) amide derivatives were generated according to Scheme 1. 2-fluoro-5-nitroaniline 1 reacted with dimethylamine to generate compound 2, and amination of compound 2 with appropriate acid chloride generated the corresponding products 3a-h. Compound 4 was developed from a previously reported procedure.[28-31] First, n-(tert-butoxycarbonyl)-4-piperidone was treated with ethyl cyanoacetate and S_8 through a Gewald reaction. Then, the compound reacted with formamidine acetate to

form a pyrimidine ring. Finally, the product was chlorinated using phosphorus oxychloride and was converted to intermediate 4.

After obtaining the key intermediates 4 and 3a-h, the nitro-compounds 3a-h were reduced by zinc powder, NH_4Cl and CH_3COOH at 80□ to generate amino-compounds without further purification which were then coupled with chloride 4 in isopropyl alcohol overnight. This was followed by Boc deprotection under acidic conditions to give the desired compounds 5a-h. Finally, the compounds 5a-h were converted to the corresponding target product 6a-p through alkylation using various substituted halogen compounds and 7a-k through amide condensation reaction using various substituted aromatic acids.

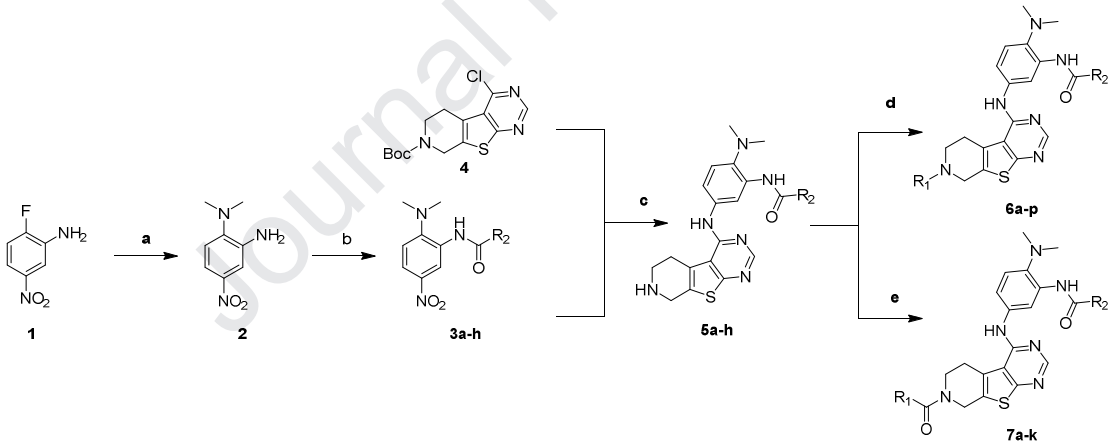

Scheme 1. Synthesis of novel TNNI3K inhibitors. Reagents and conditions: (a) Dimethylamine, EtOH at RT for 15d. (b) RCOCl, DCM, Et3N at RT for 1h, (c) (1) Zn, NH4Cl, CH_3COOH, EtOH at 80□ for 3h, (2) Isopropyl alcohol, HCl at 85□ overnight, (3) TFA, DCM at RT for 30min, (d) R-X, DIEA, EtOH at 80□ overnight. (e) RCOOH, HATU, DIEA, DCM at RT for 30 min.

2.2 The SAR (structure-activity relationship) analysis and binding modes of novel TNNI3K inhibitors

The kinase inhibitory abilities of the compounds **6a-p and 7a-k** are shown in **Table 1**, including the percentage of 1.0 μM inhibitor incubated with TNNI3K, EGFR, HER2, Flt1(VEGFR1) and KDR(VEGFR2) kinase activity. **Table 1** shows the comparison between the bioactivities of different R^1 and R^2 fragments based on the pyrido[4,5]thieno[2,3-d]pyrimidine scaffold. We utilized EGFRs and VEGFRs as models to test the off-target efficiency of synthesized compounds. The results of the kinase inhibitory assays suggest that all compounds have few off-target activities to EGFRs and VEGFRs. Moreover, results from our study suggest that a moderate steric volume at R^2 position is favorable to TNNI3K inhibition. For example, the naphthyl or 4-methylphenyl groups resulted in low inhibitory capacities on TNNI3K. Additionally, the 2-furyl or 2-thienyl substitutions at the R^2 position demonstrate better inhibitory capacities than the other substitutions (also see Figure S1). A panel of aromatic carboxyl substitutions on R^1 position were prepared and their kinase inhibitory capacities were tested. However, these aromatic carboxyl substitutions at the R^1 position did not display better TNNI3K inhibition or kinase selectivity compared to alkylation substitutions. The alkyl chains with a positively charged terminal group at R^1 position demonstrated better TNNI3K inhibitory activities compared to simple alkyl or aromatic substitutions.

The 11 compounds with better TNNI3K inhibition at 1.0μM were further evaluated for their half-inhibitory concentrations on TNNI3K, as well as the cytoprotective effects on cellular proliferation of OGD H9c2 cardiomyocyte cell lines. The corresponding results are listed in **Table 2**. Compound 6o demonstrates the best inhibitory activity on TNNI3K inhibition with an IC_{50} value of 0.41 μM. Additionally, all 11 compounds exhibit potent cytoprotective effects on OGD H9c2 cells. The cell viability of OGD H9c2 cells go from 40% to 70-90% after incubation with 1.0 or

10μM TNNI3K inhibitor. Furthermore, we evaluated the off-target kinase inhibition of compound 6o using a panel of 104 kinases through the KINOMEscan® method. As shown in Table S1, after incubation with 10 μM of compound 6o, only one member of the MAP3K family, TAK1, was significantly suppressed while the other kinases showed over 50% activity. Thus, compound 6o was selected for further studies to understand the molecular mechanism and to evaluate its efficacy in *in vivo* murine myocardial infarction models.

Table 1. The remained kinase activities (%) after 1μM compounds 6a-p and 7a-k incubation on a panel of TKs.

No.	R_1	R_2	Remained kinase activities (%) @1.0μM				
			TNNI3K	EGFR	HER2	Flt1	KDR
5a	H	CH_2CH_3	46	97	102	107	92
5b	H	4-MeC_6H_4	78	108	92	96	95
5c	H	2-pyridy	42	103	98	96	95
5d	H	3-pyridy	45	108	107	104	90
5e	H	4-pyridy	39	90	109	103	92
5f	H	1-naphthyl	71	110	90	105	88
5g	H	2-furyl	35	100	91	96	92
5h	H	2-thienyl	38	93	106	101	95
6a	CH_3	CH_2CH_3	49	99	109	95	82
6b	CH_2CH_3	CH_2CH_3	53	93	90	109	80
6c	Bn	CH_2CH_3	48	91	94	106	85
6d	2-pyrimidinyl	CH_2CH_3	59	102	99	106	80
6e	CH_3	4-MeC_6H_4	71	108	92	97	83
6f	CH_3	2-pyridy	55	100	103	94	89
6g	CH_3	3-pyridy	47	105	93	103	94
6h	CH_3	4-pyridy	46	105	97	105	84
6i	CH_3	1-naphthyl	77	98	96	101	87
6j	CH_3	2-furyl	37	93	95	105	89
6k	CH_3	2-thienyl	40	104	103	108	89

6l	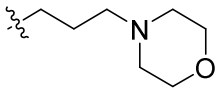	CH_2CH_3	37	105	108	90	86
6m	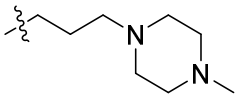	2-furyl	33	90	107	100	88
6n	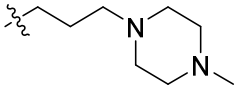	2-thienyl	38	86	103	98	93
6o	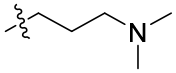	2-furyl	28	81	96	91	80
6p	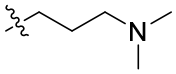	2-thienyl	33	86	102	98	81
7a	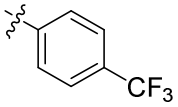	CH_2CH_3	41	107	103	109	95
7b	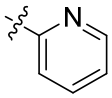	2-furyl	39	104	89	86	77
7c	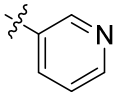	2-furyl	41	110	101	89	93
7d	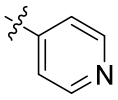	2-furyl	35	107	116	109	92
7e	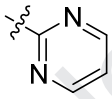	2-furyl	54	82	98	101	81
7f	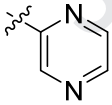	2-furyl	43	89	96	98	90
7g	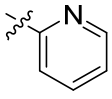	2-thienyl	40	99	99	87	73
7h	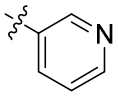	2-thienyl	45	94	93	81	69
7i	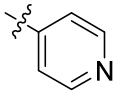	2-thienyl	36	85	110	85	82
7j	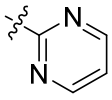	2-thienyl	49	92	112	104	86

7k		2-thienyl	44	80	113	98	80

Compound 6o was docked into the ATP site of TNNI3K by using CDOCKER module of Accelrys Discovery Studio 3.5 packages. The crystalized structure of TNNI3K kinase domain was retrieved from Protein Databank (PDB No. 4YFF), the protein preparation and molecular docking were according to the software operating manuals. The 3D and 2D contours of compound 6o bound to the ATP sites of TNNI3K are shown in **Figure 2A** and **2B**, respectively. We speculate that the N1 atom of the pyrimidine ring forms stable hydrogen bonds with the Ile542 residue, and the oxygen atom of the furan-carboxylic group forms a hydrogen bond with Thr539 of TNNI3K, respectively. Moreover, the thieno[2,3-*d*] pyrimidine scaffold forms pi-pi stack interactions with the Tyr541 residue. These interactions were similar to those of the co-crystalized TNNI3K inhibitor.

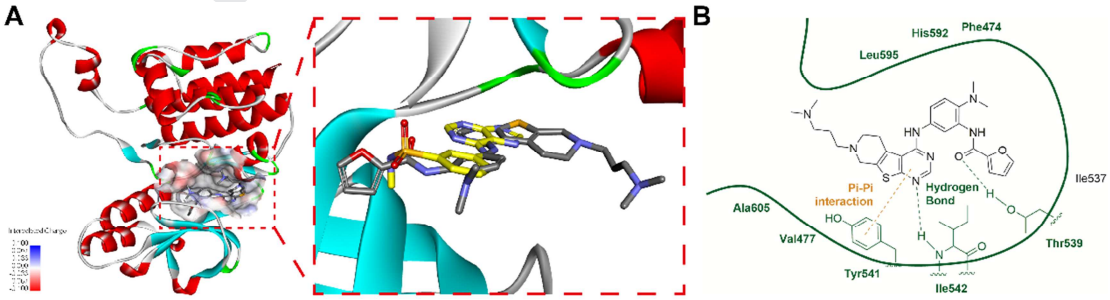

Figure 2. The 3D contour (A) and 2D contour (B) of the binding mode of compound 6o in ATP site of TNNI3K.

Table 2. The IC_{50} values (μM) of selected compounds on TNNI3K and their cytoprotective effects on OGD H9c2 cells.

No.	TNNI3K IC_{50}(μM)	Cell viability (% of control)		
		0 μM	1.0 μM	10 μM
5e	0.96±0.09	49.11±5.94	52.97±8.10	68.13±5.56
5g	0.73±0.10	47.98±7.01	54.15±8.27	71.01±8.83
5h	0.78±0.08	44.98±3.73	56.85±6.59	75.88±12.45
6j	0.56±0.04	42.40±4.32	59.62±6.13	85.56±7.90
6l	0.48±0.06	45.53±6.64	62.41±6.69	82.18±11.17
6m	0.64±0.07	42.08±4.58	61.08±6.48	79.86±6.63
6n	0.33±0.03	46.22±6.47	69.07±5.20	81.78±8.17
6o	0.24±0.03	46.02±4.55	73.82±7.80	88.95±7.84
6p	0.57±0.05	46.58±4.42	58.51±4.17	78.51±5.49
7b	0.82±0.08	42.74±4.70	54.33±6.23	70.94±10.07
7d	0.98±0.07	44.62±4.37	49.14±5.74	70.68±5.27

2.3 Novel TNNI3K inhibitor 6o efficiently suppressed ROS accumulation, apoptotic and pyroptotic cell death in oxygen and glucose deprivation (OGD) induced H9c2 cells via the p38-MAPK signaling pathway.

To evaluate the role of TNNI3K inhibitor 6o on cell death of cardiomyocytes, we focused on the effect of 6o on cell apoptosis in OGD-induced H9c2 rat cardiomyocytes. Apoptosis was determined mainly by the Annexin-V/PI dual-staining apoptosis assay, MTT method, LDH activity detection, as well as western blotting of apoptosis and pyroptosis biomarkers.[32-34] It was observed that compound 6o remarkably alleviated OGD-induced apoptosis in H9c2 rat cardiomyocytes in a dosage-dependent manner, based on Annexin-V/PI dual-staining apoptosis assay and LDH cytotoxicity assay (Figure 3A-B). Meanwhile, cytochrome C levels were

significantly decreased under the dose-dependent condition of compound 6o (Figure 3C), which further indicated that compound 6o could inhibit the mitochondrial apoptosis pathway.

TNNI3K is a member of the MAP3K superfamily according to structural homology.[15] It has been reported that TNNI3K specifically activates the p38 pathway in cardiomyocytes.[16] Therefore, we examined the activation of the classic MAPK cascade in OGD-induced H9c2 rat cardiomyocytes under a dose-dependent condition of compound 6o. Western blot analysis shows that treatment with compound 6o declined the phosphorylation levels of p38, while protein expression of total TNNI3K and p38 were not affected (Figure 3E). Moreover, no significant differences were found in the extracellular signal regulated kinase 1/2 (ERK 1/2), c-Jun N-terminal kinase (JNK) and their activation pathway (Figure 3E). These results indicate that compound 6o is capable of specifically reducing activation of the p38-MAPK pathway and myocardial cell death. Pyroptoisis can be achieved by activating the Caspase-1 pathway. NOD like receptor pyrin domain-containing protein 3 (NLRP3) binds the adaptor protein ASC and recruits Caspase-1 precursor to form the NLRP3 inflammasome, leading to the activation of Caspase-1.[35-40]

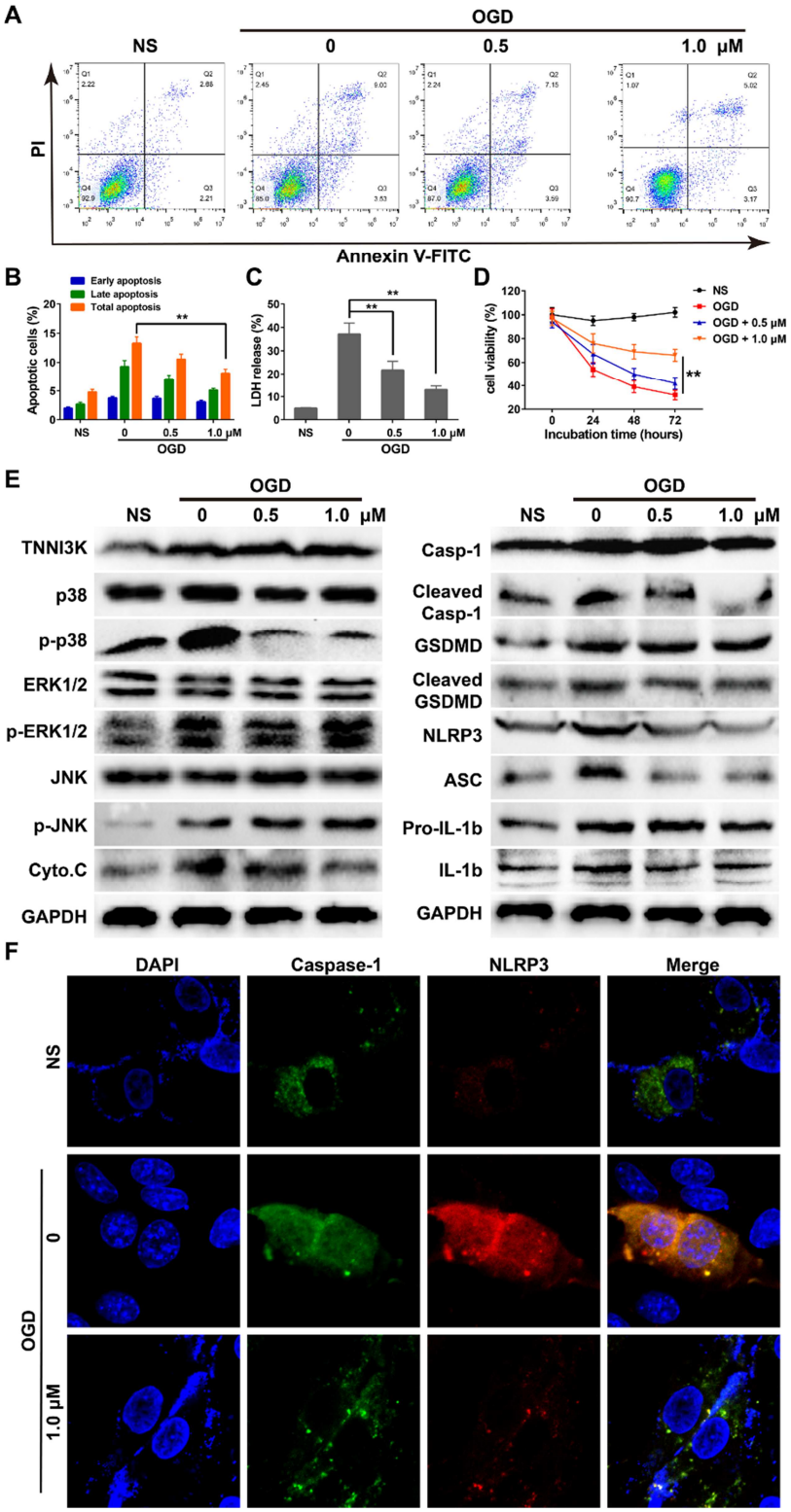

Figure 3. (A) and (B) Apoptosis in ODG-induced H9c2 cells incubated with 0.5 or 1.0 μM compound **6o** for 24h, based on dual staining with annexin-V/propidium iodide (PI) followed by flow cytometry. (C) LDH activity detection in ODG-induced H9c2 cells incubated with 0.5 or 1.0 μM compound **6o** for 24h. (D) Cell viability of ODG-induced H9c2 cells treated with 0.5 or 1.0 μM compound **6o** was assayed using the 3-(4,5-dimethylthiazol-2-yl)-2,5-diphenyltetrazolium bromide (MTT) method. $^{**}p < 0.01$. (E) Levels of TNNI3K, apoptosis-, and pyroptoisis-related proteins and phosphorylation status of

ERK1/2, JNK1/2, or p38 MAPK in ODG-induced H9c2 cells incubated with 0.5 or 1.0 μM compound **6o** assessed using Western blotting. (F) Intracellular distribution of caspase-1 and NLRP3 were detected by immunofluorescent assay.

On the one hand, activated Caspase-1 cleaves GSDMD, causing an inflammatory reaction. Additionally, it cleaves the precursors of IL-1β and IL-18 to form active IL-1β and IL-18, which cause inflammatory cells to aggregate and expand the inflammatory response.[41-44] We observed that compound 6o reduced the activation caspase-1 and GSDMD without affecting the total protein levels of caspase-1 and GSDMD. Furthermore, we observed inflammasome-associated pyroptoisis. Protein levels of NLRP3, ASC and IL-1β were significantly reduced after incubation with compound 6o, while pro-IL-1β showed no significant difference. Similarly, fluorescence microscopy showed a significant decrease in protein expression and intracellular co-localization between caspase-1 and NLRP3, indicating a potential mechanism of action between TNNI3K inhibitor and pyroptosis.

2.4 *In vivo* myocardial ischemia model and preliminary safety evaluation

An *in vivo* model of myocardial infarction in C57BL/6 male mice was established to evaluate the therapeutic efficacy of compound 6o on myocardial infarction at a dose of 25mg/kg per mice. TTC staining was used to stain mice hearts, in which the infarct area of LV stained yellow-white and the living myocardium appeared red. We observed less yellow-white area of the compound 6o-treated group compared to the NS group. In comparison to the NS group, the compound 6o-treated group showed less collagen deposition in the LV, as indicated by the size of blue region in Masson, indicating a striking decreasing levels of scar tissue.[45-47] Meanwhile, results from H&E and MT staining were consistent. Compared to the NS group, compound 6o-treated group showed fewer left ventricular inflammatory cells and significantly inhibited ventricular dilatation.

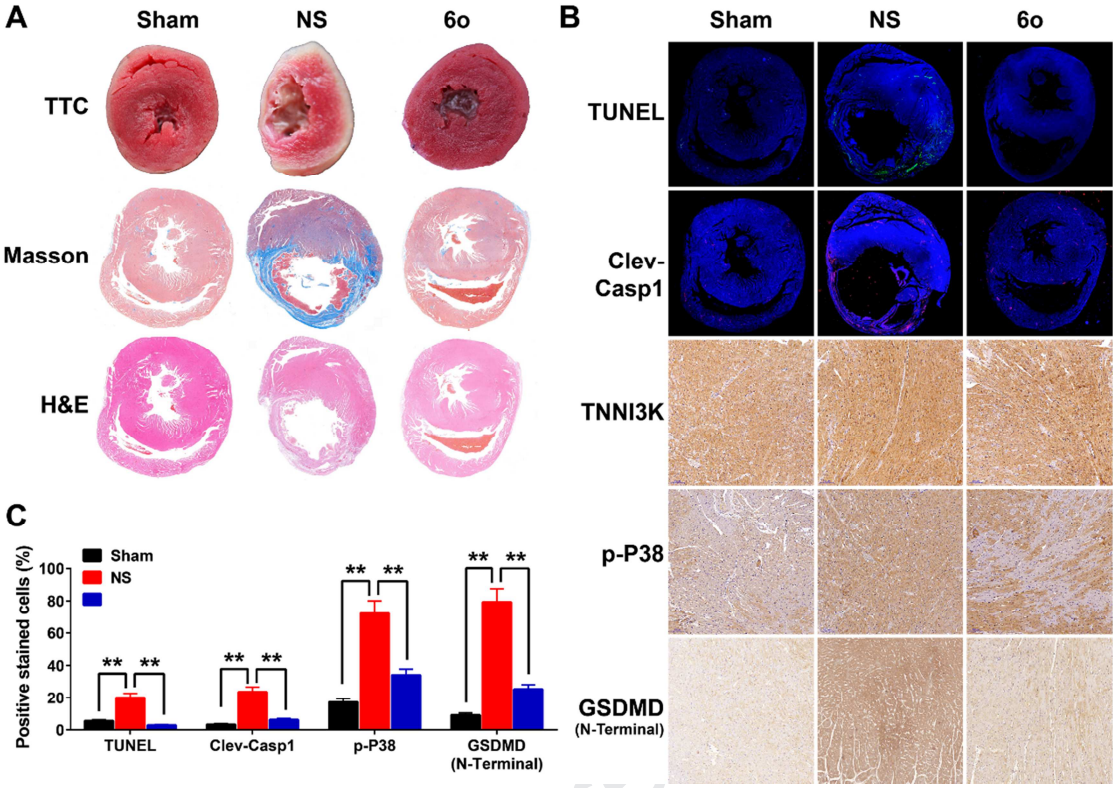

Figure 4. (A) TTC, Masson's trichrome and H&E staining of heart sections. (B) IF or IHC analysis of expression TUNEL, cleaved Caspase-1, TNNI3K, phosphorylated P38 and GSDMD (N-terminal) in the heart sections of different groups after treatment for 28 days. (C) The quantitative analysis of positive stained cells in (B).

We further analyzed the myocardial tissue after MI using immunofluorescence and immunohistochemistry to verify whether compound 6o-regulated myocardial cell recovery was related to TNNI3K inhibition and apoptosis/pyroptosis alleviation. Immunofluorescent TUNEL assay was used to detect apoptosis in LV and caspase 1 activation. The results showed that less $TUNEL^{+}$ signals (green) were observed within the LV area in compound **6o**-treated group compared to the NS group, indicating that the NS group had more left ventricular myocardial cell apoptosis, a larger infarction area, and a decrease in the activation level of caspase. Furthermore, immunohistochemical staining showed that the expression of TNNI3K, p-p38 and GSDMD was decreased. Results of the *in vivo* experiments indicated that compound

6o has a protective effect on cardiomyocytes and showed an inhibitory effect on TNNI3K. These results have demonstrated that the potential mechanism of action between TNNI3K inhibitors and pyroptosis, with results of the *in vivo* experiment being consistent with those of the *in vitro* experiments. The ADME properties of compound 6o were predicted by the ADMET tools from the Discovery Studio 3.5 package. As depicted in Figure S2, the predicted $AlogP_{98}$, absorption and BBB penetration properties of compound 6o were located in the acceptable range. The H&E staining of tissue sections suggest that there were no significant changes to the morphology of main organs of mice in both the compound 6o-treated and sham groups (Figure S3). It is also worth pointing out that our results are performed with a limited number of experimental animals and need to be validated in carefully designed studies.

In conclusion, we report the design, synthesis and biological evaluation of novel TNNI3K inhibitors with a pyrido[4,5] thieno[2,3-d]pyrimidine scaffold in OGD-induced H9c2 cardiomyocyte cell lines. The most potent inhibitor, compound 6o, remarkably suppressed ROS accumulation, apoptotic and pyroptotic cell death in OGD-induced H9c2 cells. The detailed binding modes of compound 6o to TNNI3K were probed to elucidate its kinase selectivity. Furthermore, the capacity of compound 6o to suppress apoptosis and pyroptosis were validated in a model of myocardial infarction in C57BL/6 male mice. Collectively, these results indicate that compound 6o suppressed OGD-induced H9c2 cell apoptosis and pyroptosis by interfering with the p38-MAPK signaling pathway, suggesting a novel molecular mechanism of these novel TNNI3K inhibitors that are worth further study.

3. Experimental section

3.1 Materials and Regents

The antibodies targeted towards GSDMD, NLRP3, Caspase-1, Caspase-3, Cytochrome C, p38MAPK, JNK, ERK1/2 and TUNEL assay kit were purchased from the Proteintech Group Inc. (Wuhan, China). Antibodies targeted against TNNI3K, CTnI, and the phosphorylated forms of CTnI, p38MAPK, JNK and ERK1/2 were obtained from Abcam (Cambridge, MA). The horseradish peroxidase(HRP)-labeled secondary antibodies were obtained from Cell Signal Technology (Boston, USA).

3.2 Chemical synthesis

All materials and solvents were purchased commercially. The purity of reagents was greater than 95% and could be used directly without further purification. Anhydrous reagents were processed by conventional methods or purchased directly. Column chromatography performed on silica gel (300-400 mesh) and thin-layer chromatography silica gel plate were both purchased from the Qingdao Marine Chemical Co., Ltd (Qingdao, Shandong, China) in order to purify the products. TLC, carried out on glass-backed silica plates, was visualized with UV light and I_2. Bruker Avance III 400 MHz spectrometers were used to record all ^{1}H NMR spectra. ^{13}C NMR dates were collected at 100MHz with the same instrument using TMS as an internal standard in $CDCl_3$. The δ ppm scale relative to TMS was used to describe the chemical shifts. ESI-HRMS spectrum was determined with Waters SYNAPT G2 spectrometer.

*N-(2-(dimethylamino)-5-((5,6,7,8-tetrahydropyrido[4',3':4,5]thieno[2,3-d]pyrimidin-4-yl)amino)phenyl)propionamide (**5a**)* as a white solid (yield 54%), m.p.: 94.6-102.0 □. ^{1}H NMR (400 MHz, Chloroform-*d*) δ 8.60 (br s, 1H), 8.49 (s, 1H), 8.36 (d, *J* = 2.4 Hz, 1H), 7.76 (dd, *J* = 8.8, 2.4 Hz, 1H), 7.22 (d, *J* = 8.8 Hz, 1H), 7.03 (br. s, 1H), 4.10 (t, *J* = 2.0 Hz, 2H), 3.28 (t, *J* = 5.6 Hz, 2H), 3.06 (m, 2H), 2.65 (s, 6H), 2.47 (q, *J* = 7.6 Hz, 2H), 1.28 (t, *J* = 7.6 Hz, 3H). ^{13}C NMR (101 MHz, Chloroform-*d*) δ 172.24, 166.28 , 155.17 , 152.80 , 138.76 , 135.14 , 134.00 , 133.54 , 123.79 , 120.60 , 116.91 , 116.42 , 112.23 , 45.15 , 45.00 (2C) , 42.90 , 31.13 , 27.40 , 9.70 . HRMS (ESI) *m/z* calculated for $C_{20}H_{25}N_6OS^+[M+H]^+$ 397.1805, found 397.1807.

N-(2-(dimethylamino)-5-((5,6,7,8-tetrahydropyrido[4',3':4,5]thieno[2,3-d]pyrimi

*din-4-yl)amino)phenyl)-4-methylbenzamide (**5b**)* as a white solid (yield 51%), m.p.: 195.0-197.1 □. ^{1}H NMR (400 MHz, Chloroform-*d*) δ δ 9.47 (br s, 1H), 8.52 (d, *J* = 2.4 Hz, 1H), 8.51 (s, 1H), 7.85 – 7.78 (m, 3H), 7.32 (d, *J* = 8.0 Hz, 2H), 7.27 (d, *J* = 8.8 Hz, 1H), 7.09 (br. s, 1H), 4.10 (t, *J* = 2.0 Hz, 2H), 3.30 (t, *J* = 5.6 Hz, 2H), 3.09 (m, 2H), 2.71 (s, 6H), 2.44 (s, 3H). ^{13}C NMR (101 MHz, Chloroform-*d*) δ 166.31 , 165.21 , 155.19 , 152.81 , 142.45 , 139.24 , 135.30 , 134.18 , 133.56 , 132.16 , 129.53 (2C) , 127.02 (2C) , 123.83 , 120.68 , 117.14 , 116.46 , 112.26 , 45.16 (3C) , 42.92 , 27.43 , 21.52 . HRMS (ESI) *m/z* calculated for $C_{25}H_{27}N_6OS^+$[M+H] $^+$ 459.1962, found 459.1965.

*N-(2-(dimethylamino)-5-((5,6,7,8-tetrahydropyrido[4',3':4,5]thieno[2,3-d]pyrimi din-4-yl)amino)phenyl)picolinamide (**5c**)* as a white solid (yield 56%), m.p.: 210.5-216.9 □. ^{1}H NMR (400 MHz, Chloroform-*d*) δ 11.03 (br s, 1H), 8.69 (dd, *J* = 5.6, 1.6 Hz , 1H), 8.59 (d, *J* = 2.4 Hz, 1H), 8.52 (s, 1H), 8.30 (d, *J* = 8.0 Hz, 1H), 7.91 (td, *J* = 8.0, 1.6 Hz, 1H), 7.79 (dd, *J* = 8.8, 2.4 Hz, 1H), 7.48 (m, 1H), 7.24 (d, 1H), 7.07 (br. s, 1H), 4.12 (t, *J* = 2.0 Hz, 2H), 3.31 (t, *J* = 5.6 Hz, 2H), 3.10 (m, 2H), 2.76 (s, 6H). ^{13}C NMR (101 MHz, Chloroform-*d*) δ 166.31 , 162.30 , 155.26 , 152.89 , 150.39 , 148.41 , 140.26 , 137.49 , 134.58 , 133.49 , 133.32 , 126.29 , 123.82 , 122.36 , 120.27 , 117.63 , 116.41 , 112.74 , 45.18 , 44.82 , 42.95 , 27.46 . HRMS (ESI) *m/z* calculated for $C_{23}H_{24}N_7OS^+$ [M+H] $^+$ 446.1758, found 446.1763.

*N-(2-(dimethylamino)-5-((5,6,7,8-tetrahydropyrido[4',3':4,5]thieno[2,3-d]pyrimi din-4-yl)amino)phenyl)nicotinamide (**5d**)* as a yellow solid (yield 52%), m.p.: 186.6-190.7 □. ^{1}H NMR (400 MHz, Chloroform-*d*) δ 9.62 (br s, 1H), 9.15 (d, *J* = 2.0 Hz, 1H), 8.80 (dd, *J* = 4.8, 2.0 Hz, 1H), 8.55 (d, *J* = 2.4 Hz, 1H), 8.52 (s, 1H), 8.26 (dt, *J* = 8.0, 2.0 Hz, 1H), 7.79 (dd, *J* = 8.8, 2.4 Hz, 1H), 7.49 (dd, *J* = 8.0, 4.8 Hz, 1H), 7.31 (d, *J* = 8.8 Hz, 1H), 7.09 (br. s, 1H), 4.13 (d, *J* = 2.0 Hz, 2H), 3.32 (t, *J* = 5.6 Hz, 2H), 3.12 (d, *J* = 5.6 Hz, 2H), 2.72 (s, 6H). ^{13}C NMR (101 MHz, Chloroform-*d*) δ 166.40 , 163.23 , 155.12 , 152.79 , 152.57 , 147.90 , 139.29 , 135.48 , 135.24 , 133.73 , 133.63 , 130.69 , 123.79 , 123.75 , 120.98 , 117.72 , 116.47 , 112.33 , 45.25 , 45.15 , 42.91 , 27.40 . HRMS (ESI) *m/z* calculated for $C_{23}H_{24}N_7OS^+$[M+H] $^+$ 446.1758, found 446.1765.

*N-(2-(dimethylamino)-5-((5,6,7,8-tetrahydropyrido[4',3':4,5]thieno[2,3-d]pyrimidin-4-yl)amino)phenyl)isonicotinamide (**5e**)* as a white solid (yield 55%), m.p.: 220.3-223.0 □. 1H NMR (400 MHz, Chloroform-d) δ 9.63 (br s, 1H), 8.88 – 8.83 (m, 2H), 8.55 (d, *J* = 2.4 Hz, 1H), 8.52 (s, 1H), 7.79 (dd, *J* = 8.8, 2.4 Hz, 1H), 7.76 – 7.73 (m, 2H), 7.31 (d, *J* = 8.8 Hz, 1H), 7.09 (br s, 1H), 4.12 (t, *J* = 2.0 Hz, 2H), 3.31 (t, *J* = 5.6 Hz, 2H), 3.10 (m, 2H), 2.73 (s, 6H). ^{13}C NMR (101 MHz, Chloroform-*d*) δ 166.41 , 163.04 , 155.09 , 152.75 , 150.88 (2C) , 141.97 , 139.32 , 135.51 , 133.77 , 133.45 , 123.73 , 120.97 , 120.75 (2C) , 117.94 , 166.48 , 112.38 , 45.26 (2C) , 45.17 , 42.92 , 27.43 . HRMS (ESI) m/z calculated for $C_{23}H_{24}N_7OS^+$[M+H] $^+$ 446.1758, found 446.1761.

*N-(2-(dimethylamino)-5-((5,6,7,8-tetrahydropyrido[4',3':4,5]thieno[2,3-d]pyrimidin-4-yl)amino)phenyl)-1-naphthamide (**5f**)* as a grey solid (yield 63%), m.p.: 129.5-135.6 □. ^{1}H NMR (400 MHz, Chloroform-*d*) δ 9.20 (br s, 1H), 8.67 (d, *J* = 2.4 Hz, 1H), 8.53 (s, 1H), 8.44 (dd, *J* = 7.2, 2.4 Hz, 1H), 7.97 (d, *J* = 8.0 Hz, 1H), 7.91 (dd, *J* = 7.2, 2.4Hz, 1H), 7.82 (dd, *J* = 8.8, 2.4 Hz, 1H), 7.75 (dd, *J* = 6.8, 1.2 Hz, 1H), 7.60 – 7.50 (m, 3H), 7.28 (d, *J* = 8.8 Hz, 1H), 7.14 (br s, 1H), 4.08 (t, *J* = 2.0 Hz, 2H), 3.29 (t, *J* = 5.6 Hz, 2H), 3.09 (m, 2H), 2.63 (s, 6H). ^{13}C NMR (101 MHz, Chloroform-*d*) δ 167.60 , 166.38 , 155.22 , 152.80 , 139.26 , 135.38 , 134.63 , 134.35 , 133.83 , 133.58 , 131.09 , 130.20 , 128.46 , 127.30 , 126.59 , 125.35 , 125.10 , 124.82 , 123.86 , 120.92 , 117.61 , 116.52 , 112.47 , 45.16 (3C) , 42.93 , 27.40 . HRMS (ESI) *m/z* calculated for $C_{28}H_{27}N_6OS^+$[M+H] $^+$ 495.1962, found 495.1963.

*N-(2-(dimethylamino)-5-((5,6,7,8-tetrahydropyrido[4',3':4,5]thieno[2,3-d]pyrimidin-4-yl)amino)phenyl)furan-2-carboxamide (**5g**)* as a grey solid (yield 57%), m.p.: 207.7-213.1 □. ^{1}H NMR (400 MHz, Chloroform-*d*) δ 9.54 (br s, 1H), 8.50 (s, 1H), 8.48 (d, *J* = 2.4 Hz, 1H), 7.79 (dd, *J* = 8.8, 2.4 Hz, 1H), 7.57 (dd, *J* = 1.6, 0.8 Hz, 1H), 7.25 (d, *J* = 8.8 Hz, 1H), 7.23 (dd, *J* = 3.6, 0.8 Hz, 1H), 7.06 (br s, 1H), 6.57 (dd, *J* = 3.6, 1.6 Hz, 1H), 4.10 (t, *J* = 2.0 Hz, 2H), 3.29 (t, *J* = 5.6 Hz, 2H), 3.08 (m, 2H), 2.72 (s, 6H). ^{13}C NMR (101 MHz, Chloroform-*d*) δ 166.30 , 156.20 , 155.14 , 152.80 , 148.23 , 144.47 , 139.32 , 135.10 , 133.50 , 133.48 , 123.79 , 120.65 , 117.32 , 116.43 ,

115.11 , 112.51 , 112.33 , 45.13 , 45.03 (2C) , 42.89 , 27.36 . HRMS (ESI) *m/z* calculated for $C_{22}H_{23}N_6O_2S^+[M+H]^+$ 435.1598, found 435.1605

*N-(2-(dimethylamino)-5-((5,6,7,8-tetrahydropyrido[4',3':4,5]thieno[2,3-d]pyrimidin-4-yl)amino)phenyl)thiophene-2-carboxamide (**5h**)* as a grey solid (yield 65%), m.p.: 201.6-207.1 □. ^{1}H NMR (400 MHz, Chloroform-*d*) δ 9.35 (br s, 1H), 8.51 (s, 1H), 8.43 (d, *J* = 2.4 Hz, 1H), 7.82 (dd, *J* = 8.8, 2.4 Hz, 1H), 7.63 (dd, *J* = 3.6, 1.2 Hz, 1H), 7.56 (dd, *J* = 5.2, 1.2 Hz, 1H), 7.26 (d, *J* = 8.8 Hz, 1H), 7.16 (dd, *J* = 5.2, 3.6 Hz, 1H), 7.08 (s, 1H), 4.11 (t, *J* = 2.0 Hz, 2H), 3.30 (t, *J* = 5.6 Hz, 2H), 3.08 (m, 2H), 2.72 (s, 6H). ^{13}C NMR (101 MHz, Chloroform-*d*) δ 166.33, 159.78 , 155.12 , 152.80 , 139.80 , 138.98 , 135.37 , 133.79 , 133.49 , 130.84 , 128.30 , 127.94 , 123.79 , 120.72 , 117.17 , 116.44 , 112.10 , 45.16 , 45.12 , 42.88 , 27.35 . HRMS (ESI) *m/z* calculated for $C_{22}H_{23}N_6OS_2^+[M+H]^+$ 451.1369, found 451.1371.

*N-(2-(dimethylamino)-5-((7-methyl-5,6,7,8-tetrahydropyrido[4',3':4,5]thieno[2,3-d]pyrimidin-4-yl)amino)phenyl)propionamide (**6a**)* as a white solid (yield 70%), m.p.: 124.6-127.6 □. ^{1}H NMR (400 MHz, Chloroform-*d*) δ 8.60 (br s, 1H), 8.50 (s, 1H), 8.37 (d, *J* = 2.4 Hz, 1H), 7.78 (dd, *J* = 8.8, 2.4 Hz, 1H), 7.22 (d, *J* = 8.8 Hz, 1H), 7.02 (br s, 1H), 3.71 (t, *J* = 2.0 Hz, 2H), 3.16 (m, 2H), 2.89 (t, *J* = 5.6 Hz, 2H), 2.65 (s, 6H), 2.54 (s, 3H), 2.47 (q, *J* = 7.6 Hz, 2H), 1.28 (t, *J* = 7.6 Hz, 3H). ^{13}C NMR (101 MHz, Chloroform-*d*) δ 172.21, 166.57 , 155.16 , 152.90 , 138.73 , 135.17 , 134.03 , 131.71 , 123.16 , 120.60 , 116.89 , 116.02 , 112.20 , 54.02 , 51.64 , 45.27 , 45.01 (2C) , 31.12 , 26.72 , 9.69 . HRMS (ESI) *m/z* calculated for $C_{21}H_{27}N_6OS^+[M+H]^+$ 411.1962, found 411.1961.

*N-(2-(dimethylamino)-5-((7-ethyl-5,6,7,8-tetrahydropyrido[4',3':4,5]thieno[2,3-d]pyrimidin-4-yl)amino)phenyl)propionamide (**6b**)* as a white solid (yield 69%), m.p.: 125.1-128.6 □. 1H NMR (400 MHz, Chloroform-d) δ 8.60 (br s, 1H), 8.50 (s, 1H), 8.37 (d, *J* = 2.4 Hz, 1H), 7.79 (dd, *J* = 8.8, 2.4 Hz, 1H), 7.22 (d, *J* = 8.8 Hz, 1H), 7.02 (br s, 1H), 3.77 (t, *J* = 2.0 Hz, 2H), 3.16 (m, 2H), 2.94 (t, *J* = 5.6 Hz, 2H), 2.69 (q, *J* = 7.2 Hz, 2H), 2.65 (s, 6H), 2.47 (q, *J* = 7.6 Hz, 2H), 1.28 (t, *J* = 7.6 Hz, 3H), 1.22 (t, *J* = 7.2 Hz, 3H). ^{13}C NMR (101 MHz, Chloroform-*d*) δ 172.20 , 166.59 , 155.12 , 152.90 , 138.68 , 135.23 , 134.05 , 132.00 , 123.57 , 120.62 , 116.77 , 116.04 , 112.09 ,

51.83 , 51.27 , 49.43 , 45.02 (2C) , 31.13 , 26.79 , 12.54 , 9.68 . HRMS (ESI) *m/z* calculated for $C_{22}H_{29}N_6OS^+[M+H]^+$ 425.2118, found 425.2115.

*N-(5-((7-benzyl-5,6,7,8-tetrahydropyrido[4',3':4,5]thieno[2,3-d]pyrimidin-4-yl)amino)-2-(dimethylamino)phenyl)propionamide (**6c**)* as a white solid (yield 64%), m.p.: 158.4-163.3 □. ^{1}H NMR (400 MHz, Chloroform-d) δ 8.59 (br. s, 1H), 8.49 (s, 1H), 8.36 (d, *J* = 2.4 Hz, 1H), 7.77 (dd, *J* = 8.6, 2.4 Hz, 1H), 7.43 – 7.28 (m, 5H), 7.21 (d, *J* = 8.6 Hz, 1H), 7.02 (br. s, 1H), 3.77 (s, 2H), 3.75 (t, *J* = 2.0 Hz, 2H), 3.16 (m, 2H), 2.96 (t, *J* = 5.6 Hz, 2H), 2.65 (s, 6H), 2.46 (q, *J* = 7.6 Hz, 2H), 1.27 (t, *J* = 7.6 Hz, 3H). ^{13}C NMR (101 MHz, Chloroform-*d*) δ 172.18 , 166.58 , 155.15 , 152.90 , 138.67 , 137.70 , 135.22 , 134.05 , 131.99 , 129.02 (2C) , 128.51 (2C) , 127.47 , 123.57 , 120.61 , 116.75 , 116.10 , 112.11 , 61.68 , 52.05 , 49.47 , 45.02 (2C) , 31.13 , 26.70 , 9.69 . HRMS (ESI) *m/z* calculated for $C_{27}H_{31}N_6OS^+[M+H]^+$ 487.2275, found 487.2283.

*N-(2-(dimethylamino)-5-((7-(pyrimidin-2-yl)-5,6,7,8-tetrahydropyrido[4',3':4,5]thieno[2,3-d]pyrimidin-4-yl)amino)phenyl)propionamide (**6d**)* as a white solid (yield 54%), mp: 158.4-163.3 □. ^{1}H NMR (400 MHz, Chloroform-*d*) δ 8.58 (br s, 1H), 8.50 (s, 1H), 8.40 (d, *J* = 2.4 Hz, 1H), 8.37 (d, *J* = 4.8 Hz, 2H), 7.69 (dd, *J* = 8.8, 2.4 Hz, 1H), 7.21 (d, *J* = 8.8 Hz, 1H), 7.00 (br s, 1H), 6.57 (t, *J* = 4.8 Hz, 1H), 5.10 (t, *J* = 2.0 Hz, 2H), 4.28 (t, *J* = 5.6 Hz, 2H), 3.22 (m , 2H), 2.65 (s, 6H), 2.47 (q, *J* = 7.6 Hz, 2H), 1.27 (t, *J* = 7.6 Hz, 3H). ^{13}C NMR (101 MHz, Chloroform-*d*) δ 172.16 , 166.75 , 161.46 , 157.92 (2C) , 155.17 , 153.01 , 138.81 , 135.06 , 134.06 , 131.94 , 124.30 , 120.58 , 116.89 , 116.12 , 112.35 , 110.76 , 45.00 (2C) , 44.04 , 40.97 , 31.14 , 26.03 , 9.70 . HRMS (ESI) *m/z* calculated for $C_{24}H_{27}N_8OS^+[M+H]^+$ 475.2023, found 475.2028.

*N-(2-(dimethylamino)-5-((7-methyl-5,6,7,8-tetrahydropyrido[4',3':4,5]thieno[2,3-d]pyrimidin-4-yl)amino)phenyl)-4-methylbenzamide (**6e**)* as a orange solid (yield 73%), m.p.: 105.6-109.7 □. ^{1}H NMR (400 MHz, Chloroform-*d*) δ 9.48 (br s, 1H), 8.52 (d, *J* = 2.4 Hz, 1H), 8.51 (s, 1H), 7.86 - 7.77 (m, 3H), 7.32 (d, *J* = 8.0 Hz, 2H), 7.27 (d, *J* = 8.8 Hz, 1H), 7.08 (br s, 1H), 3.71 (t, *J* = 2.0 Hz, 2H), 3.20 (m, 2H), 2.90 (t, *J* = 5.6 Hz, 2H), 2.71 (s, 6H), 2.54 (s, 3H), 2.44 (s, 3H). ^{13}C NMR (101 MHz,

Chloroform-*d*) δ 166.58 , 165.20 , 155.18 , 152.91 , 142.43 , 139.23 , 135.31 , 134.19 , 132.18 , 131.70 , 129.52 (2C) , 127.03 (2C) , 123.20 , 120.68 , 117.14 , 116.06 , 112.27 , 54.01 , 51.65 , 45.26 , 45.17 (2C) , 26.73 , 21.52 . HRMS (ESI) *m/z* calculated for $C_{26}H_{29}N_6OS^+$[M+H] $^+$ 473.2118, found 473.2120.

*N-(2-(dimethylamino)-5-((7-methyl-5,6,7,8-tetrahydropyrido[4',3':4,5]thieno[2,3-d]pyrimidin-4-yl)amino)phenyl)picolinamide (**6f**)* as a light-yellow solid (yield 79%), m.p.: 105.6-110.2 □. ^{1}H NMR (400 MHz, Chloroform-*d*) δ 11.03 (br s, 1H), 8.69 (m, 1H), 8.59 (d, *J* = 2.4 Hz, 1H), 8.52 (s, 1H), 8.30 (dt, *J* = 8.0, 1.2 Hz, 1H), 7.91 (td, *J* = 8.0, 1.6 Hz, 1H), 7.79 (dd, *J* = 8.8, 2.4 Hz, 1H), 7.48 (m, 1H), 7.25 (d, *J* = 8.8 Hz, 1H), 7.07 (br s, 1H), 3.72 (t, *J* = 2.0 Hz, 2H), 3.20 (m, 2H), 2.90 (t, *J* = 5.6 Hz, 2H), 2.76 (s, 6H), 2.54 (s, 3H). ^{13}C NMR (101 MHz, Chloroform-*d*) δ 166.55 , 162.29 , 155.25 , 152.96 , 150.38 , 148.41 , 140.26 , 137.48 , 134.58 , 133.30 , 131.59 , 126.29 , 123.22 , 122.35 , 120.25 , 117.66 , 116.01 , 112.78 , 54.00 , 51.65 , 45.25 , 44.82 (2C) , 26.71 . HRMS (ESI) *m/z* calculated for $C_{24}H_{26}N_7OS^+$[M+H] $^+$ 460.1914, found 460.1923.

*N-(2-(dimethylamino)-5-((7-methyl-5,6,7,8-tetrahydropyrido[4',3':4,5]thieno[2,3-d]pyrimidin-4-yl)amino)phenyl)nicotinamide (**6g**)* as a white solid (yield 78%), m.p.: 209.8-211.9 □. ^{1}H NMR (400 MHz, Chloroform-*d*) δ 9.62 (br s, 1H), 9.15 (d, *J* = 2.0 Hz, 1H), 8.80 (dd, *J* = 4.8, 2.0 Hz, 1H), 8.55 (d, *J* = 2.4 Hz, 1H), 8.53 (s, 1H), 8.26 (dt, *J* = 8.0, 2.0 Hz, 1H), 7.80 (dd, *J* = 8.8, 2.4 Hz, 1H), 7.49 (dd, *J* = 8.0, 4.8 Hz, 1H), 7.30 (d, *J* = 8.8 Hz, 1H), 7.07 (br s, 1H), 3.73 (t, *J* = 2.0 Hz, 2H), 3.21 (m, 2H), 2.91 (t, *J* = 5.6 Hz, 2H), 2.72 (s, 6H), 2.55 (s, 3H). ^{13}C NMR (101 MHz, Chloroform-*d*) δ 166.67, 163.21 , 155.11 , 152.87 , 152.57 , 147.91 , 139.26 , 135.50 , 135.23 , 133.74 , 131.84 , 130.70 , 123.78 , 123.13 , 120.97 , 117.70 , 116.07 , 112.31 , 54.01 , 51.65 , 45.28 (2C) , 45.25 , 26.74 . HRMS (ESI) *m/z* calculated for $C_{24}H_{26}N_7OS^+$[M+H] $^+$ 460.1914, found 460.1913.

*N-(2-(dimethylamino)-5-((7-methyl-5,6,7,8-tetrahydropyrido[4',3':4,5]thieno[2,3-d]pyrimidin-4-yl)amino)phenyl)isonicotinamide (**6h**)* as a white solid (yield 73%), mp: 221.4-224.3 □. ^{1}H NMR (400 MHz, Chloroform-*d*) δ 9.63 (br s, 1H), 8.88 – 8.81 (m, 2H), 8.55 (d, *J* = 2.4 Hz, 1H), 8.53 (s, 1H), 7.80 (dd, *J* = 8.8, 2.4 Hz, 1H), 7.77 – 7.71 (m, 2H), 7.31 (d, *J* = 8.8 Hz, 1H), 7.07 (br s, 1H), 3.72 (t, *J* = 2.0 Hz, 2H), 3.20

(m, 2H), 2.91 (t, *J* = 5.6 Hz, 2H), 2.73 (s, 6H), 2.55 (s, 3H). ^{13}C NMR (101 MHz, Chloroform-*d*) δ 116.70 , 163.04 , 155.09 , 152.85 , 150.89 (2C) , 141.99 , 139.31 , 135.53 , 133.47 , 131.94 , 123.11 , 120.98 , 120.76 (2C) , 117.96 , 116.09 , 112.39 , 54.03 , 51.66 , 45.30 (2C) , 45.27 , 26.76 . HRMS (ESI) *m/z* calculated for $C_{24}H_{26}N_7OS^+$ [M + H] $^+$ 460.1914, found 460.1917.

N-(2-(dimethylamino)-5-((7-methyl-5,6,7,8-tetrahydropyrido[4',3':4,5]thieno[2,3-d]pyrimidin-4-yl)amino)phenyl)-1-naphthamide ***(6i)*** as a light-yellow solid (yield 60%), m.p.: 118.7-125.0 □. ^{1}H NMR (400 MHz, Chloroform-*d*) δ 9.20 (br s, 1H), 8.66 (d, *J* = 2.4 Hz, 1H), 8.53 (s, 1H), 8.45 (dd, *J* = 7.2, 2.4 Hz, 1H), 8.00 (d, *J* = 8.0 Hz, 1H), 7.92(dd, *J* = 7.2, 2.4 Hz, 1H), 7.82 (dd, *J* = 8.8, 2.4 Hz, 1H), 7.77 (dd, *J* = 6.8, 1.2 Hz, 1H), 7.62 – 7.51 (m, 3H), 7.29 (d, *J* = 8.8 Hz, 1H), 7.12 (br s, 1H), 3.73 (t, *J* = 2.0 Hz, 2H), 3.22 (t, *J* = 5.6 Hz, 2H), 2.91 (t, *J* = 5.6 Hz, 2H), 2.64 (s, 6H), 2.55 (s, 3H). ^{13}C NMR (101 MHz, Chloroform-*d*) δ 167.60 , 166.65, 155.24 , 152.92 , 139.30 , 135.34 , 134.66 , 134.36 , 133.85 , 131.76 , 131.10 , 130.23 , 128.45 , 127.32 , 126.60 , 125.37 , 125.12 , 124.85 , 123.22 , 120.93 , 117.68 , 116.10 , 112.53 , 54.03 , 51.67 , 45.28 , 45.16 (2C) , 26.75 . HRMS (ESI) *m/z* calculated for $C_{29}H_{28}N_6NaOS^+$ [M + Na] $^+$ 531.1938, found 531.1942.

N-(2-(dimethylamino)-5-((7-methyl-5,6,7,8-tetrahydropyrido[4',3':4,5]thieno[2,3-d]pyrimidin-4-yl)amino)phenyl)furan-2-carboxamide ***(6j)*** as a white solid (yield 78%), m.p.: 159.1-160.3 □. ^{1}H NMR (400 MHz, Chloroform-*d*) δ 9.55 (br s, 1H), 8.51 (s, 1H), 8.48 (d, *J* = 2.4 Hz, 1H), 7.81 (dd, *J* = 8.8, 2.4 Hz, 1H), 7.57 (dd, *J* = 1.6, 0.8 Hz, 1H), 7.26 (d, *J* = 8.8 Hz, 1H), 7.24 (dd, *J* = 3.6, 0.8 Hz, 1H), 7.05 (br s, 1H), 6.57 (dd, *J* = 3.6, 1.6 Hz, 1H), 3.71 (t, *J* = 2.0 Hz, 2H), 3.18 (m, 2H), 2.89 (t, *J* = 5.6 Hz, 2H), 2.72 (s, 6H), 2.54 (s, 3H). ^{13}C NMR (101 MHz, Chloroform-*d*) δ 166.59 , 156.18 , 155.13 , 152.90 , 148.27 , 144.43 , 139.30 , 135.13 , 133.52 , 131.75 , 123.16 , 120.65 , 117.30 , 116.04 , 115.08 , 112.49 , 112.32 , 54.02 , 51.65 , 45.28 , 45.04 (2C) , 26.73 . HRMS (ESI) *m/z* calculated for $C_{23}H_{25}N_6O_2S^+$ [M + H] $^+$ 449.1754, found 449.1757.

N-(2-(dimethylamino)-5-((7-methyl-5,6,7,8-tetrahydropyrido[4',3':4,5]thieno[2,3-d]pyrimidin-4-yl)amino)phenyl)thiophene-2-carboxamide ***(6k)*** as a white solid (yield

75%), m.p.: 101.3-105.0 □. ^{1}H NMR (400 MHz, Chloroform-*d*) δ 9.37 (br s, 1H), 8.52 (s, 1H), 8.43 (d, *J* = 2.4 Hz, 1H), 7.85 (dd, *J* = 8.8, 2.4 Hz, 1H), 7.64 (dd, *J* = 3.6, 1.2 Hz, 1H), 7.57 (dd, *J* = 5.2, 1.2 Hz, 1H), 7.28 (d, *J* = 8.8 Hz , 1H), 7.16 (dd, *J* = 5.2, 3.6 Hz, 1H), 7.06 (s, 1H), 3.72 (t, *J* = 2.0 Hz, 2H), 3.18 (m, 2H), 2.90 (t, *J* = 5.6 Hz, 2H), 2.72 (s, 6H), 2.54 (s, 3H). ^{13}C NMR (101 MHz, Chloroform-*d*) δ 166.61 , 159.77 , 155.11 , 152.89 , 139.84 , 138.96 , 135.39 , 133.82 , 131.79 , 130.82 , 128.29 , 127.92 , 123.15 , 120.73 , 117.15 , 116.06 , 112.10 , 54.02 , 51.65 , 45.27 , 45.17 (2C) , 26.73 . HRMS (ESI) *m/z* calculated for $C_{23}H_{25}N_6OS_2^+$ [M + H] $^+$ 465.1526, found 465.1528.

N-(2-(dimethylamino)-5-((7-(3-morpholinopropyl)-5,6,7,8-tetrahydropyrido[4',3' :4,5]thieno[2,3-d]pyrimidin-4-yl)amino)phenyl)propionamide ***(6l)*** as pink solid (yield 45%), m.p.: 118.1-122.5. ^{1}H NMR (400 MHz, Chloroform-*d*) δ 8.60 (br s, 1H), 8.50 (s, 1H), 8.36 (d, *J* = 2.4 Hz, 1H), 7.79 (dd, *J* = 8.8, 2.4 Hz, 1H), 7.22 (d, *J* = 8.8 Hz, 1H), 7.02 (br s, 1H), 3.76 (t, *J* = 2.0 Hz, 2H) , 3.73 (t, *J* = 4.8 Hz, 4H), 3.15 (t, *J* = 5.6 Hz, 2H), 2.94 (t, *J* = 5.6 Hz, 2H), 2.65 (m, 8H), 2.53 – 2.39 (m, 8H), 1.79 (q, *J* = 7.6 Hz, 2H), 1.28 (t, *J* = 7.6 Hz, 3H). ^{13}C NMR (101 MHz, Chloroform-*d*) δ 172.24 , 166.55 , 155.14 , 152.91 , 138.72 , 135.18 , 134.03 , 131.88 , 123.57 , 120.62 , 116.82 , 116.04 , 112.12 , 67.00 (2C) , 56.86 , 55.24 , 53.80 (2C) , 52.25 , 49.73 , 45.02 (2C) , 31.12 , 26.64 , 24.52 , 9.68 . HRMS (ESI) *m/z* calculated for $C_{27}H_{38}N_7O_2S^+$ [M + H] $^+$ 524.2802, found 524.2806.

N-(2-(dimethylamino)-5-((7-(3-(4-methylpiperazin-1-yl)propyl)-5,6,7,8-tetrahydr opyrido[4',3':4,5]thieno[2,3-d]pyrimidin-4-yl)amino)phenyl)furan-2-carboxamide ***(6m)*** as a red solid (yield 35%), m.p.: 90.5-97.1 □. ^{1}H NMR (400 MHz, Chloroform-*d*) δ 9.55 (br s, 1H), 8.51 (s, 1H), 8.47 (d, *J* = 2.4 Hz, 1H), 7.81 (dd, *J* = 8.8, 2.4 Hz, 1H), 7.57 (dd, *J* = 1.6, 0.8 Hz, 1H), 7.26 (d, *J* = 8.8 Hz, 1H), 7.24 (dd, *J* = 3.6, 0.8 Hz, 1H), 7.05 (br s, 1H), 6.57 (dd, *J* = 3.6, 1.6 Hz, 1H), 3.77 (t, *J* = 2.0 Hz, 2H), 3.16 (t, *J* = 5.6 Hz, 2H), 2.95 (t, *J* = 5.6 Hz, 2H), 2.72 (s, 6H), 2.65 (t, *J* = 7.6 Hz, 2H), 2.62 – 2.33 (m, 10H), 2.29 (s, 3H), 1.81 (p, *J* = 7.6 Hz, 2H). ^{13}C NMR (101 MHz, Chloroform-*d*) δ 166.58 , 159.78 , 155.09 , 152.87 , 139.82 , 138.94 , 135.39 , 133.81 , 132.01 , 130.82 , 128.29 , 127.92 , 123.56 , 120.73 , 117.11 , 116.08 , 112.07 , 56.42 , 55.36 , 55.12

(2C) , 53.25 (2C) , 52.21 , 49.75 , 46.03 , 45.17 (2C) , 26.64 , 24.84 . HRMS (ESI) *m/z* calculated for $C_{30}H_{39}N_8O_2S^+$ $[M + H]^+$ 575.2911, found 575.2910.

*N-(2-(dimethylamino)-5-((7-(3-(4-methylpiperazin-1-yl)propyl)-5,6,7,8-tetrahydropyrido[4',3':4,5]thieno[2,3-d]pyrimidin-4-yl)amino)phenyl)thiophene-2-carboxamide (**6n**)* as a white solid (yield 37%), m.p.: 48.9-55.7 □. ^{1}H NMR (400 MHz, Chloroform-*d*) δ 9.38 (br s, 1H), 8.52 (s, 1H), 8.44 (d, *J* = 2.4 Hz, 1H), 7.86 (dd, *J* = 8.8, 2.4 Hz, 1H), 7.65 (dd, *J* = 3.6, 1.2 Hz, 1H), 7.58 (dd, *J* = 5.2, 1.2 Hz, 1H), 7.28 (d , *J* = 8.8 Hz, 1H), 7.17 (dd, *J* = 5.2, 3.6 Hz, 1H), 7.08 (s, 1H), 3.78 (t, *J* = 2.0 Hz, 2H), 3.17 (t, *J* = 5.6 Hz, 2H), 2.96 (t, *J* = 5.6 Hz, 2H), 2.74 (s, 6H), 2.66 (t, *J* = 7.6 Hz, 2H), 2.63 – 2.34 (m, 10H), 2.31 (s, 3H), 1.82 (p, *J* = 7.6 Hz, 2H). ^{13}C NMR (101 MHz, Chloroform-*d*) δ 166.53 , 159.70 , 155.03 , 152.81 , 139.81 , 138.87 , 135.38 , 133.76 , 131.97 , 130.80 , 128.23 , 127.90 , 123.56 , 120.67 , 117.02 , 116.04 , 112.00 , 56.39 , 55.34 , 55.10 (2C) , 53.22 (2C) , 52.19 , 49.72 , 46.02 , 45.14 (2C) , 26.63 , 24.83 . HRMS (ESI) *m/z* calculated for $C_{30}H_{39}N_8OS_2^+$ $[M + H]^+$ 591.2683, found 591.2681.

*N-(2-(dimethylamino)-5-((7-(3-(dimethylamino)propyl)-5,6,7,8-tetrahydropyrido[4',3':4,5]thieno[2,3-d]pyrimidin-4-yl)amino)phenyl)furan-2-carboxamide (**6o**)* as a white solid (yield 40%), m.p.: 64.9-70.5 □. ^{1}H NMR (400 MHz, Chloroform-*d*) δ 9.55 (br s, 1H), 8.51 (s, 1H), 8.48 (d, *J* = 2.4 Hz, 1H), 7.81 (dd, *J* = 8.8, 2.4 Hz, 1H), 7.57 (dd, *J* = 1.6, 0.8 Hz, 1H), 7.26 (d, *J* = 8.8 Hz, 1H), 7.24 (dd, *J* = 3.6, 0.8 Hz, 1H), 7.06 (br s, 1H), 6.57 (dd, *J* = 3.6, 1.6 Hz, 1H), 3.77 (t, *J* = 2.0 Hz, 2H), 3.17 (m, 2H), 2.95 (t, *J* = 5.6 Hz, 2H), 2.72 (s, 6H), 2.65 (t, *J* = 7.6 Hz , 2H), 2.41 (t, *J* = 7.6 Hz , 2H), 2.28 (s, 6H), 1.80 (p, *J* = 7.6 Hz, 2H). ^{13}C NMR (101 MHz, Chloroform-*d*) δ 166.59 , 156.18 , 155.11 , 152.90 , 148.27 , 144.43 , 139.27 , 135.15 , 133.53 , 131.95 , 123.58 , 120.66 , 117.23 , 116.05 , 115.07 , 112.49 , 112.26 , 57.60 , 55.26 , 52.28 , 49.74 , 45.36 (2C) , 45.04 (2C) , 26.70 , 25.39 . HRMS (ESI) *m/z* calculated for $C_{27}H_{34}N_7O_2S^+$ $[M + H]^+$ 520.2489, found 520.2486.

*N-(2-(dimethylamino)-5-((7-(3-(dimethylamino)propyl)-5,6,7,8-tetrahydropyrido[4',3':4,5]thieno[2,3-d]pyrimidin-4-yl)amino)phenyl)thiophene-2-carboxamide (**6p**)* as a white solid (yield 40%), m.p.: 39.8-43.5 □. ^{1}H NMR (400 MHz, Chloroform-*d*) δ 9.36 (br s, 1H), 8.51 (s, 1H), 8.44 (d, *J* = 2.4 Hz, 1H), 7.84 (dd, *J* = 8.8, 2.4 Hz, 1H),

7.64 (d, *J* = 3.6 Hz, 1H), 7.56 (d, *J* = 5.2 Hz, 1H), 7.27 (d , *J* = 8.8 Hz , 1H), 7.16 (dd, *J* = 5.2, 3.6 Hz, 1H), 7.07 (br s, 1H), 3.77 (t, *J* = 2.0 Hz, 2H), 3.16 (t, *J* = 5.6 Hz, 2H), 2.95 (t, *J* = 5.6 Hz, 2H), 2.72 (s, 6H), 2.65 (t, *J* = 7.6 Hz, 2H), 2.39 (t, *J* = 7.6 Hz, 2H), 2.27 (s, 6H), 1.79 (p, *J* = 7.6 Hz, 2H). ^{13}C NMR (101 MHz, Chloroform-*d*) δ 166.60 , 159.76 , 155.08 , 152.87 , 139.84 , 138.92 , 135.42 , 133.82 , 132.03 , 130.81 , 128.28 , 127.92 , 123.57 , 120.73 , 117.07 , 116.08 , 112.03 , 57.67 , 55.35 , 52.28 , 49.75 , 45.49 (2C) , 45.17 (2C) , 26.70 , 25.55 . HRMS (ESI) *m/z* calculated for $C_{27}H_{34}N_7OS_2^+$ [M + H] $^+$ 536.2261, found 536.2252.

*N-(2-(dimethylamino)-5-((7-(4-(trifluoromethyl)benzoyl)-5,6,7,8-tetrahydropyrido[4',3':4,5]thieno[2,3-d]pyrimidin-4-yl)amino)phenyl)propionamide (**7a**)* as a light yellow (yield 85%), m.p.: 208.1-210.6. ^{1}H NMR (400 MHz, Chloroform-*d*) δ 8.59 (br s, 1H), 8.55 – 8.22 (m, 2H), 7.87 – 7.52 (m, 5H), 7.22 (d, *J* = 8.8 Hz, 1H), 6.98, 6.90 (2br s, rotamers, 1H), 5.02, 4.69 (2s, rotamers, 2H), 4.17, 3.80 (2s, rotamers, 2H), 3.28, 3.17 (2s, rotamers, 2H), 2.65 (s, 6H), 2.47 (q, *J* = 7.6 Hz, 2H), 1.27 (t, *J* = 7.6 Hz, 3H). ^{13}C NMR (101 MHz, Chloroform-*d*) δ 172.29 , 169.37 , 166.98 , 155.21 , 153.35 , 139.01 , 138.69 , 134.84 , 134.05 , 132.30 (q, *J* = 30 Hz, 1C) , 127.46 – 127.34 (m, 2C) , 126.35 (q, *J* = 273 Hz, 1C), 125.96 (2C) , 122.28 , 120.64 , 117.15 , 116.93 , 115.73 , 112.04 , 44.98 (2C) , 44.43, 42.33 , 31.12 , 27.33 , 9.67 . HRMS (ESI) *m/z* calculated for $C_{28}H_{28}F_3N_6O_2S^+$ [M + H] $^+$ 569.1941, found 569.1937.

*N-(2-(dimethylamino)-5-((7-picolinoyl-5,6,7,8-tetrahydropyrido[4',3':4,5]thieno[2,3-d]pyrimidin-4-yl)amino)phenyl)furan-2-carboxamide (**7b**)* as a light yellow (yield 86%), m.p.: 124.5-132.2 □. ^{1}H NMR (400 MHz, Chloroform-*d*) δ 9.57, 9.54(2 br s, rotamers, 1H), 8.69, 8.64 (2d, *J* =4.8 Hz, rotamers, 1H), 8.61 – 8.38 (m, 2H), 7.89 – 7.60 (m, 3H), 7.57 (s, 1H), 7.46 – 7.38 (m, 1H), 7.28, 7.27(2s, rotamers, 1H), 7.26 – 7.22(m, 1H), 7.02, 7.01 (2s, rotamers, 1H), 6.58 (dd, *J* = 3.5, 1.8 Hz, 1H), 5.06, 5.03 (2s, rotamers, 2H), 4.22, 4.05 (2t, *J* = 5.6 Hz, rotamers, 2H), 3.32 (t, *J* = 5.6 Hz, 2H), 2.74 (s, 6H). ^{13}C NMR (101 MHz, Chloroform-d) δ 167.71 , 166.96 , 156.24 , 155.15 , 153.37 , 153.30 , 153.13 , 148.46 , 148.26 , 148.19 , 144.53 , 137.30 , 133.47 , 130.36 , 125.10 , 124.80 , 124.40 , 123.93 , 120.68 , 117.49 , 115.95 , 115.12 , 112.50 , 45.03

(2C) , 44.38 , 42.70 , 27.50 . HRMS (ESI) *m/z* calculated for $C_{28}H_{25}N_7NaO_3S^+$ [M + Na] $^+$ 562.1632, found 562.1630.

*N-(2-(dimethylamino)-5-((7-nicotinoyl-5,6,7,8-tetrahydropyrido[4',3':4,5]thieno[2,3-d]pyrimidin-4-yl)amino)phenyl)furan-2-carboxamide (**7c**)* as a light yellow (yield 77%), m.p.: 127.5-130.1 □. ^{1}H NMR (400 MHz, Chloroform-*d*) δ 9.51 (br s, 1H), 8.77 (br s, 1H), 8.74 (dd, *J* = 4.8, 1.6 Hz 2H), 8.64 – 8.35 (m, 2H), 7.84 (dt, *J* = 8.0, 2.0 Hz, 1H), 7.74, 7.63 (2s, rotamers, 1H), 7.58 – 7.54 (m, 1H), 7.43 (t, *J* = 6.0 Hz, 1H), 7.25 (d, *J* = 8.8 Hz, 1H), 7.22 (d, *J* = 3.6 Hz, 1H), 7.12 – 6.89 (m, 1H), 6.57 (dd, *J* = 3.6, 1.6 Hz, 1H), 5.02, 4.78 (2s, rotamers, 2H), 4.16, 3.86 (2s, rotamers, 2H), 3.24 (s, 2H), 2.72 (s, 6H). ^{13}C NMR (101 MHz, Chloroform-*d*) δ 168.26 , 166.99 , 156.14 , 155.25 , 153.36 , 151.39 , 148.19 , 148.01 , 144.48 , 139.58 , 134.79 , 133.51 , 131.08 , 130.09 , 123.64 , 120.64 , 117.49 , 115.77 , 115.12 , 112.51 , 44.99 (3C) , 42.45 , 29.70 . HRMS (ESI) *m/z* calculated for $C_{28}H_{25}N_7NaO_3S^+$ [M + Na] $^+$ 562.1632, found 562.1630.

*N-(2-(dimethylamino)-5-((7-isonicotinoyl-5,6,7,8-tetrahydropyrido[4',3':4,5]thieno[2,3-d]pyrimidin-4-yl)amino)phenyl)furan-2-carboxamide (**7d**)* as a light yellow (yield 90%), m.p.: 134.1-137.5 □. ^{1}H NMR (400 MHz, Chloroform-*d*) δ 9.53 (br s, 1H), 8.86 – 8.71 (m, 2H), 8.61 – 8.36 (m, 2H), 7.72, 7.62 (2d, *J* = 8.4 Hz, rotamers, 1H), 7.59 – 7.54 (m,1H), 7.26 (d, *J* = 8.8 Hz, 2H), 7.23 (d, *J* = 3.2 Hz, 1H), 7.01, 6.90 (2s, rotamers, 1H), 6.58 (dd, *J* = 3.6, 1.6 Hz, 1H), 5.03, 4.67 (2s, rotamers, 2H), 4.19, 3.79 (2s, rotamers, 2H), 3.31, 3.18 (2s, rotamers, 2H), 2.72 (s, 6H). ^{13}C NMR (101 MHz, Chloroform-*d*) δ 168.20 , 167.05 , 156.19 , 155.15 , 153.32 , 150.61 (2C) , 148.15 , 144.52 , 142.82 , 139.56 , 134.76 , 133.51 , 130.00 , 123.16 , 121.02 , 120.66 , 117.49 , 115.72 , 115.16 (2C) , 112.53 , 112.34 , 44.99 (2C) , 44.27 , 42.16 , 27.26 . HRMS (ESI) *m/z* calculated for $C_{28}H_{25}N_7NaO_3S^+$ [M + Na] $^+$ 562.1632, found 562.1632.

*N-(2-(dimethylamino)-5-((7-(pyrimidine-2-carbonyl)-5,6,7,8-tetrahydropyrido[4',3':4,5]thieno[2,3-d]pyrimidin-4-yl)amino)phenyl)furan-2-carboxamide (**7e**)* as a light yellow (yield 93%), m.p.: 151.7-157.1 □. ^{1}H NMR (400 MHz, Chloroform-*d*) δ 9.56, 9.54 (2br s, 1H), 8.92, 8.87 (2d, *J* = 4.8 Hz, rotamers, 2H), 8.63 – 8.33 (m, 2H), 7.94 –

7.56 (m, 2H), 7.45, 7.42 (2t, *J* = 4.8 Hz, rotamers, 1H), 7.30 – 7.27 (m, 1H), 7.26 – 7.21 (m, 1H), 7.02, 6.97 (2s, rotamers, 1H), 6.58 (dd, *J* = 3.6, 1.6 Hz, 1H), 5.10, 4.75 (2t, *J* = 2.0 Hz, rotamers, 2H), 4.25, 3.80 (2t, *J* = 6.0 Hz, rotamers, 2H), 3.33, 3.28 (2t, *J* = 6.0 Hz, rotamers, 2H), 2.73 (s, 6H). ^{13}C NMR (101 MHz, Chloroform-*d*) δ 167.00 , 165.29 , 161.58 , 157.61 (2C) , 156.24 , 155.10 , 153.16 , 148.14 , 144.56 , 135.03 , 133.43 , 129.94 , 129.18 , 124.71 , 123.65 , 121.64 , 120.70 , 117.35 , 115.86 , 115.09 , 112.50 , 45.03 (2C) , 43.94 , 42.08 , 27.18 . HRMS (ESI) *m/z* calculated for $C_{27}H_{24}N_8NaO_3S^+$ [M + Na] $^+$ 563.1584, found 563.1581.

*N-(2-(dimethylamino)-5-((7-(pyrazine-2-carbonyl)-5,6,7,8-tetrahydropyrido[4',3' :4,5]thieno[2,3-d]pyrimidin-4-yl)amino)phenyl)furan-2-carboxamide (**7f**)* as a light yellow (yield 92%), m.p.: 121.9-126.7 □. ^{1}H NMR (400 MHz, Chloroform-*d*) δ 9.56, 9.52 (2s, rotamers, 1H), 9.08 (d, *J* = 1.6 Hz, 1H), 8.72, 8.70 (2d, *J* = 2.4 Hz, rotamers, 1H), 8.66 – 8.41 (m, 3H), 7.85, 7.62 (2dd, rotamers, *J* = 8.8, 2.4 Hz, 1H), 7.57 (t, *J* = 2.8 Hz, 1H), 7.27 – 7.22 (m, 2H), 7.04, 7.01 (2s, rotamers, 1H), 6.58 (dd, *J* = 3.6, 1.6 Hz, 1H), 5.06, 5.05 (2s, rotamers, 2H), 4.22, 4.07 (2t, *J* = 5.6 Hz, rotamers, 2H), 3.34 (t, *J* = 5.6 Hz, 2H), 2.73 (s, 6H). ^{13}C NMR (101 MHz, Chloroform-*d*) δ 167.01 , 165.34 , 156.26 , 155.16 , 153.22 , 148.55 , 148.16 , 146.49 , 146.25 , 145.96 , 144.56 , 142.56 , 139.44 , 134.95 , 133.48 , 129.96 , 124.50 , 123.85 , 120.70 , 117.50 , 115.15 , 112.52 , 45.03 (2C) , 44.44 , 42.89 , 27.51 . HRMS (ESI) *m/z* calculated for $C_{27}H_{24}N_8NaO_3S^+$ [M + Na] $^+$ 563.1584, found 563.1582.

*N-(2-(dimethylamino)-5-((7-picolinoyl-5,6,7,8-tetrahydropyrido[4',3':4,5]thieno [2,3-d]pyrimidin-4-yl)amino)phenyl)thiophene-2-carboxamide (**7g**)* as a light yellow (yield 91%), m.p.: 123.7-130.5 □. ^{1}H NMR (400 MHz, Chloroform-*d*) δ 9.37, 9.32 (2s, rotamers, 1H), 8.67 (2d, *J* = 4.8 Hz, rotamers, 1H), 8.59 – 8.35 (m, 2H), 7.90 – 7.61 (m, 4H), 7.57 (dd, *J* = 5.2, 1.6 Hz, 1H), 7.45 – 7.38 (m, 1H), 7.29 – 7.25 (m, 1H), 7.16 (dd, *J* = 4.8, 3.6 Hz, 1H), 7.03, 7.01 (2br s, rotamers, 1H), 5.06, 5.03 (2s, rotamers, 2H), 4.22, 4.05 (2t, *J* = 5.6 Hz, rotamers, 2H), 3.32 (d, *J* = 5.6 Hz, 2H), 2.72 (s, 6H). ^{13}C NMR (101 MHz, Chloroform-*d*) δ 167.72 , 166.96 , 159.79 , 155.11 , 153.36 , 153.10 , 148.49 , 139.77 , 139.06 , 137.29 , 135.25 , 133.76 , 130.88 , 130.32 , 128.28 , 127.96 , 125.09 , 124.35 , 123.96 , 120.72 , 117.26 , 115.97 , 112.08 , 45.15

(2C) , 44.36 , 42.67 , 27.47 . HRMS (ESI) *m/z* calculated for $C_{28}H_{25}N_7NaO_2S_2^+$ [M + Na] $^+$ 578.1403, found 578.1404.

*N-(2-(dimethylamino)-5-((7-nicotinoyl-5,6,7,8-tetrahydropyrido[4',3':4,5]thieno [2,3-d]pyrimidin-4-yl)amino)phenyl)thiophene-2-carboxamide (**7h**)* as a light yellow (yield 90%), m.p.: 135.5-141.8 □. ^{1}H NMR (400 MHz, Chloroform-*d*) δ 9.31 (s, 1H), 8.76 (s, 1H), 8.72 (dd, *J* = 5.2, 1.6 Hz, 1H), 8.56 – 8.37 (m, 2H), 7.84 (d, *J* = 8.0 Hz, 1H), 7.79 – 7.58 (m, 2H), 7.55 (dd, *J* = 5.2, 1.2 Hz, 1H), 7.41 (t, *J* = 6.4 Hz, 1H), 7.24 (d, *J* = 8.8 Hz, 1H), 7.14 (dd, *J* = 4.8, 3.6 Hz, 1H), 7.03 (br s, 1H), 5.00, 4.76(2s, rotamers, 2H), 4.15, 3.84 (2s, rotamers, 2H), 3.24 (s, 2H), 2.71 (s, 6H). ^{13}C NMR (101 MHz, Chloroform-*d*) δ 168.25 , 166.97 , 159.70 , 155.19 , 153.28 , 151.36 , 147.98 , 139.72 , 139.21 , 135.07 , 133.75 , 131.10 , 130.88 , 128.27 , 127.94 , 123.64 , 120.67 , 117.33 , 115.81 , 112.28 , 45.11 (2C) , 44.62 , 42.47 , 27.21 . HRMS (ESI) *m/z* calculated for $C_{28}H_{25}N_7NaO_2S_2^+$ [M + Na] $^+$ 578.1403, found 578.1403.

*N-(2-(dimethylamino)-5-((7-isonicotinoyl-5,6,7,8-tetrahydropyrido[4',3':4,5]thie no[2,3-d]pyrimidin-4-yl)amino)phenyl)thiophene-2-carboxamide (**7i**)* as a light yellow (yield 90%), m.p.: 129.0-134.1 □. ^{1}H NMR (400 MHz, Chloroform-*d*) δ 9.35 (br s, 1H), 8.85 – 8.70 (m, 2H), 8.58 – 8.28 (m, 2H), 7.91 – 7.60 (m, 2H), 7.57 (dd, *J* = 4.8, 1.2 Hz, 1H), 7.44 – 7.31 (m, 2H), 7.27 (d, *J* = 8.8 Hz 1H), 7.16 (dd, *J* = 4.8, 3.6 Hz, 1H), 7.02, 6.92 (2br s, rotamers, 1H), 5.03, 4.67 (2s, rotamers, 2H), 4.19, 3.80 (2s, rotamers, 2H), 3.31, 3.19 (2s, rotamers, 2H), 2.73 (s, 6H). ^{13}C NMR (101 MHz, Chloroform-*d*) δ 168.19 , 166.99 , 159.73 , 155.07, 153.20 , 150.56 (2C), 142.84 , 139.66 , 139.14 , 135.07 , 133.71 , 130.95 , 128.27 , 127.97 (2C) , 124.92 , 123.3, 121.05 , 120.65 , 117.30 , 115.76 , 112.2 , 45.11 (2C) , 44.26 , 42.14 , 27.19 . HRMS (ESI) *m/z* calculated for $C_{28}H_{25}N_7NaO_2S_2^+$ [M + Na] $^+$ 578.1403, found 578.1401.

*N-(2-(dimethylamino)-5-((7-(pyrimidine-2-carbonyl)-5,6,7,8-tetrahydropyrido[4' ,3':4,5]thieno[2,3-d]pyrimidin-4-yl)amino)phenyl)thiophene-2-carboxamide (**7j**)* as a light yellow (yield 92%), m.p.: 152.3-156.1 □. ^{1}H NMR (400 MHz, Chloroform-*d*) δ 9.38, 9.32 (2br s, rotamers, 1H), 8.92, 8.87 (2d, rotamers, 2H), 8.61 – 8.29 (m, 2H), 8.00 – 7.54 (m, 3H), 7.45, 7.41 (2t, *J* = 4.8 Hz, rotamers, 1H), 7.27 (d, *J* = 8.8 Hz, 1H), 7.19 – 7.13 (m, 1H), 7.03, 6.98 (2br s, rotamers, 1H), 5.10, 4.75 (2t, *J* = 2.0 Hz,

rotamers, 2H), 4.25, 3.81 (2t, *J* = 5.6 Hz, rotamers, 2H), 3.33, 3.27 (2t, *J* = 5.6 Hz, 2H), 2.73 (s, 6H). ^{13}C NMR (101 MHz, Chloroform-*d*) δ 167.01 , 165.30 , 161.57 , 159.82 , 157.62 (2C), 155.07 , 153.13 , 139.73 , 139.03 , 135.27 , 133.72 , 130.93 , 129.96 , 128.29 , 127.99 , 123.66 , 121.65 , 120.76 , 117.14 , 115.89 , 111.88 , 45.15 (2C) , 43.94 , 42.07 , 27.18 . HRMS (ESI) *m/z* calculated for $C_{27}H_{24}N_8NaO_2S_2^+$ [M + Na] $^+$ 579.1356, found 579.1354.

*N-(2-(dimethylamino)-5-((7-(pyrazine-2-carbonyl)-5,6,7,8-tetrahydropyrido[4',3' :4,5]thieno[2,3-d]pyrimidin-4-yl)amino)phenyl)thiophene-2-carboxamide (**7k**)* as a light yellow (yield 93%), m.p.: 118.9-123.5 □. ^{1}H NMR (400 MHz, Chloroform-*d*) δ 9.37, 9.32 (2br s, rotamers, 1H), 9.09 (d, *J* = 1.2 Hz, 1H), 8.72, 8.69 (2d, *J* = 2.4 Hz, rotamers, 1H), 8.66, 8.59 (2t, *J* = 2.0 Hz, rotamers, 1H), 8.57 – 8.35 (m, 2H), 7.92 – 7.61 (m, 2H), 7.60 – 7.53 (m, 1H), 7.30 – 7.24 (m, 1H), 7.19 – 7.12 (m, 1H), 7.04, 7.02 (2s, rotamers, 1H), 5.09 – 5.02 (m, 2H), 4.22, 4.07 (2t, *J* = 5.6 Hz, rotamers, 2H), 3.34 (t, *J* = 5.6 Hz, 2H), 2.73 (s, 6H). ^{13}C NMR (101 MHz, Chloroform-*d*) δ 167.03 , 165.36 , 159.85 , 155.13 , 153.20 , 148.55 , 146.24 , 145.97 , 142.58 , 139.7 , 139.11 , 135.21 , 133.77 , 130.94 , 129.99 , 128.32 , 127.99 , 123.84 , 120.76 , 117.29 , 115.9 , 112.03 , 45.16 , 44.44 , 42.89 , 27.51 . HRMS (ESI) *m/z* calculated for $C_{27}H_{24}N_8NaO_2S_2^+$ [M + Na] $^+$ 579.1356, found 579.1354.

3.3 Kinase assays

The Kinase Profiler services purchased from Eurofins provided the Src, EGFR and KDR kinase detection, as previously reported.[48, 49] TNNI3K-based HTRF detection was purchased by Cisbio Co. Ltd.. In short, a GST-marked kinase domain of the TNNI3K was used for HTRF detection. Subsequently, the biotinylated substrate peptide of CTnI and two HTRF assay reagents were added. The HTRF signal was related to the quantity of TNNI3K kinase domains marked by GST interacting with the biotinylated substrate peptide in direct proportion. Detailed experimental steps are reported in previous studies. The KINOMEScan® selectivity profiling was implemented by DiscoveRx Co. Ltd. based on the company's protocol and previous reports. [48]

3.4 Cell proliferation, Apoptosis and LDH activity detection

The MTT method are used to detect cellular proliferation on H9c2 cardiomyocytes treated with small molecular inhibitors. Normally, H9c2 cells are inoculated in a 96-well plate with $1x10^5$ cells per well treated with target concentration of inhibitor for 24 h. Data from three independent replicates were used to calculate the average inhibition rates. Without further description, MTT solution (5 mg/ml) was added to the H9c2 cells and incubated for 3 hours to measure cell viability. Next, the MTT solution was disposed and DMSO was added to dissolve the formazan crystals. A Thermo Multiscan Spectrum was used to determine absorbance at 570 nm. The apoptosis of H9c2 cells was assayed by Annexin V/PI dual-staining flow cytometry method. Detailed experimental procedures are provided in our previous studies. The Pierce LDH cytotoxicity detection kit (Thermo Scientific) was used in the detection of LDH in culture medium based on the manufacturer's protocol.

3.5 Western blotting

The H9c2 cells were collected, digested with trypsin and washed twice with cold PBS after treatment with saline or compound 11b under the OGD (Oxygen and glucose deprivation) atmosphere. RIPA buffer was used to lyse the cells prior to denaturation by sonication. Subsequently, the lysates were treated with a refrigerated centrifuge for 30 min and the supernatant was gathered. Then, the total protein concentration was determined. SDS-PAGE was used to isolate the gathered lysate proteins, which were then transferred to the PVDF membrane and incubated with relevant primary and secondary antibodies. Protein was visualized using the ECL Kit (enhanced chemiluminescence, Millpore, USA).

3.6 The Myocardial Ischemia Model

MI model was established using C57BL/6 male mice (5-6 weeks) bought from Beijing HFK Bioscience Co., Ltd. Animals were acclimatized at a controlled temperature of 20-22^oC, with a relative humidity of 50-60% and light-dark for 12h each. The Institutional Animal Care and Treatment Committee of Sichuan University (Chengdu, P.R. China) approved the animal experiments. As reported earlier, lasting ligation of the left anterior descending coronary artery (LAD) can lead to MI.

Ketamine (100mg /kg) and xylazine (10mg/kg) were intraperitoneally injected for anaesthetizing the animals. Tracheotomy was performed with a small animal respiratory ventilator with a tidal volume of 0.1ml and a breathing rate of 110 times/min. LV (left ventricle) was observed after opening the chest of mice, and a left intercostal thoracotomy was conducted. LAD was ligated with a 5-0 silk suture at approximately 1mm from the end of the left atrium after the pericardium removed. The significant color changes in the ischemic area may indicate a successful coronary artery occlusion of LAD. Next, 4~0 silk was used to suture the chest. On this basis, continuous ventilation was provided for 30 min at 37□ until lungs of the post-MI mice expanded again. The sham operation group performed the same procedures without blocking the LAD. The mice that suffered from MI were in the NS group, and normal saline was administered to the control group. The post-MI mice were stochastically split into three groups (Sham, NS and TNNI3K inhibitor treated groups, n=4), and intraperitoneal injected every two days. Each mouse was injected with TNNI3K inhibitor at a dose of 25 mg/kg. The sham group represented the negative control group.

3.7 Immunohistochemistry and Immunofluorescent assays

EDTA antigenic retrieval buffer (pH 8.0) or citrate buffer (pH 6.0) were used to soak the heart tissue sections, and the antigen was recovered using a microwave. Then, the slides were incubated using the homologous primary antibody for 30-40 minutes at 37□. The negative control group was the normal anti-rabbit or anti-mouse IgG. HRP polymer conjugated with the second antibody was used to treat the slides for 30 minutes and then the diaminobenzidine solution was used in immunohistochemical analysis. For Immunofluorescence (IF) detections: fluorescein bonded with secondary antibody was used to treat the slides, which then were detected under fluorescent microscope.

Acknowledgement

This work was supported by grants from National Natural Science Foundation of

China (Grant No. 21772131) and the Fundamental Research Funds for the Science & Technology department of Sichuan Province (2019YFSY0004 and 20GJHZ0179).

Supporting Information

Additional figures containing the H&E stained tissue sections of main organs, ^{1}H NMR and ^{13}C NMR spectra of synthesized compounds.

References

[1] A.S. Go, D. Mozaffarian, V.L. Roger, E.J. Benjamin, J.D. Berry, M.J. Blaha, S.F. Dai, E.S. Ford, C.S. Fox, S. Franco, H.J. Fullerton, C. Gillespie, S.M. Hailpern, J.A. Heit, V.J. Howard, M.D. Huffman, S.E. Judd, B.M. Kissela, S.J. Kittner, D.T. Lackland, J.H. Lichtman, L.D. Lisabeth, R.H. Mackey, D.J. Magid, G.M. Marcus, A. Marelli, D.B. Matchar, D.K. McGuire, E.R. Mohler, C.S. Moy, M.E. Mussolino, R.W. Neumar, G. Nichol, D.K. Pandey, N.P. Paynter, M.J. Reeves, P.D. Sorlie, J. Stein, A. Towfighi, T.N. Turan, S.S. Virani, N.D. Wong, D. Woo, M.B. Turner, S. Amer Heart Assoc Stroke, S. Stroke Statistics, Executive Summary: Heart Disease and Stroke Statistics-2014 Update A Report From the American Heart Association, Circulation, 129 (2014) 399-410.

[2] D.J. Hausenloy, D.M. Yellon, Myocardial ischemia-reperfusion injury: a neglected therapeutic target, Journal of Clinical Investigation, 123 (2013) 92-100.

[3] E. Murphy, C. Steenbergen, Mechanisms underlying acute protection from cardiac ischemia-reperfusion injury, Physiological Reviews, 88 (2008) 581-609.

[4] D.M. Yellon, D.J. Hausenloy, Mechanisms of disease: Myocardial reperfusion injury, New England Journal of Medicine, 357 (2007) 1121-1135.

[5] J. Curran, D. Burkhoff, R.A. Kloner, Beyond Reperfusion: Acute Ventricular Unloading and Cardioprotection During Myocardial Infarction, Journal of Cardiovascular Translational Research, 12 (2019) 95-106.

[6] D.J. Hausenloy, D. Garcia-Dorado, H.E. Botker, S.M. Davidson, J. Downey, F.B. Engel, R. Jennings, S. Lecour, J. Leor, R. Madonna, M. Ovize, C. Perrino, F. Prunier, R. Schulz, J.P.G. Sluijter, L.W. Van Laake, J. Vinten-Johansen, D.M. Yellon, K. Ytrehus, G. Heusch, P. Ferdinandy, Novel targets and future strategies for acute cardioprotection: Position Paper of the European Society of Cardiology Working Group on Cellular Biology of the Heart, Cardiovascular Research, 113 (2017) 564-585.

[7] R.A. Kloner, Current State of Clinical Translation of Cardioprotective Agents for Acute Myocardial Infarction, Circulation Research, 113 (2013) 451-463.

[8] A. Krzywonos-Zawadzka, A. Franczak, G. Sawicki, M. Wozniak, I. Bil-Lula, Multidrug prevention or therapy of ischemia-reperfusion injury of the heart-Mini-review, Environmental Toxicology and Pharmacology, 55 (2017) 55-59.

[9] P. Bullon, F.J. Cano-Garcia, E. Alcocer-Gomez, A. Varela-Lopez, L. Roman-Malo, R.J. Ruiz-Salmeron, J.L. Quiles, J.M. Navarro-Pando, M. Battino, J. Ruiz-Cabello, L.J. Jimenez-Borreguero, M.D. Cordero, Could NLRP3-Inflammasome Be a Cardiovascular Risk Biomarker in Acute

Myocardial Infarction Patients?, Antioxidants & Redox Signaling, 27 (2017) 269-275.
[10] T.Y. Forbes-Hernandez, F. Giampieri, M. Gasparrini, L. Mazzoni, J.L. Quiles, J.M. Alvarez-Suarez, M. Battino, The effects of bioactive compounds from plant foods on mitochondrial function: A focus on apoptotic mechanisms, Food and Chemical Toxicology, 68 (2014) 154-182.
[11] F. Giampieri, S. Afrin, T.Y. Forbes-Hernandez, M. Gasparrini, D. Cianciosi, P. Reboredo-Rodriguez, A. Varela-Lopez, J.L. Quiles, M. Battino, Autophagy in Human Health and Disease: Novel Therapeutic Opportunities, Antioxidants & Redox Signaling, 30 (2019) 577-634.
[12] P. Reboredo-Rodriguez, A. Varela-Lopez, T.Y. Forbes-Hernandez, M. Gasparrini, S. Afrin, D. Cianciosi, J.J. Zhang, P.P. Manna, S. Bompadre, J.L. Quiles, M. Battino, F. Giampieri, Phenolic Compounds Isolated from Olive Oil as Nutraceutical Tools for the Prevention and Management of Cancer and Cardiovascular Diseases, International Journal of Molecular Sciences, 19 (2018) 2305.
[13] J.J. Zhang, F. Giampieri, S. Afrin, M. Battino, X.D. Zheng, P. Reboredo-Rodriguez, Structure-stability relationship of anthocyanins under cell culture condition, International Journal of Food Sciences and Nutrition, 70 (2019) 285-293.
[14] J.J. Zhang, J.B. Xiao, F. Giampieri, T.Y. Forbes-Hernandez, M. Gasparrini, S. Afrin, D. Cianciosi, P. Reboredo-Rodriguez, M. Battino, X.D. Zheng, Inhibitory effects of anthocyanins on alpha-glucosidase activity, Journal of Berry Research, 9 (2019) 109-123.
[15] Y. Zhao, X.M. Meng, Y.J. Wei, X.W. Zhao, D.Q. Liu, H.Q. Cao, C.C. Liew, J.F. Ding, Cloning and characterization of a novel cardiac-specific kinase that interacts specifically with cardiac troponin I, Journal of Molecular Medicine-Jmm, 81 (2003) 297-304.
[16] R.J. Vagnozzi, G.J. Gatto, L.S. Kallander, N.E. Hoffman, K. Mallilankaraman, V.L.T. Ballard, B.G. Lawhorn, P. Stoy, J. Philp, A.P. Graves, Y. Naito, J.J. Lepore, E. Gao, M. Madesh, T. Force, Inhibition of the Cardiomyocyte-Specific Kinase TNNI3K Limits Oxidative Stress, Injury, and Adverse Remodeling in the Ischemic Heart, Science Translational Medicine, 5 (2013) ra141.
[17] H. Wang, L. Wang, L. Song, Y.W. Zhang, J. Ye, R.X. Xu, N. Shi, X.M. Meng, TNNI3K is a novel mediator of myofilament function and phosphorylates cardiac troponin I, Brazilian Journal of Medical and Biological Research, 46 (2013) 128-137.
[18] L. Wang, H. Wang, J. Ye, R.X. Xu, L. Song, N. Shi, Y.W. Zhang, X. Chen, X.M. Meng, Adenovirus-mediated overexpression of cardiac troponin I-interacting kinase promotes cardiomyocyte hypertrophy, Clinical and Experimental Pharmacology and Physiology, 38 (2011) 278-284.
[19] Y. Wang, S.Q. Wang, L.P. Wang, Y.H. Yao, C.Y. Ma, J.F. Ding, J. Ye, X.M. Meng, J.J. Li, R.X. Xu, Overexpression of Cardiac-Specific Kinase TNNI3K Promotes Mouse Embryonic Stem Cells Differentiation into Cardiomyocytes, Cellular Physiology and Biochemistry, 41 (2017) 381-398.
[20] H. Lal, F. Ahmad, S. Parikh, T. Force, Troponin I-Interacting Protein Kinase - A Novel Cardiac-Specific Kinase, Emerging as a Molecular Target for the Treatment of Cardiac Disease, Circulation Journal, 78 (2014) 1514-1519.
[21] H. Tang, K.H. Xiao, L. Mao, H.A. Rockman, D.A. Marchuk, Overexpression of TNNI3K, a cardiac-specific MAPKKK, promotes cardiac dysfunction, Journal of Molecular and Cellular Cardiology, 54 (2013) 101-111.
[22] D.M. Abraham, D.A. Marchuk, Inhibition of the Cardiomyocyte-Specific Troponin I-Interacting Kinase Limits Oxidative Stress, Injury, and Adverse Remodeling due to Ischemic Heart Disease, Circulation Research, 114 (2014) 938-940.
[23] A. Milano, E.M. Lodder, C.R. Bezzina, TNNI3K in cardiovascular disease and prospects for therapy, Journal of Molecular and Cellular Cardiology, 82 (2015) 167-173.

[24] B.G. Lawhorn, J. Philp, Y.D. Zhao, C. Louer, M. Hammond, M. Cheung, H. Fries, A.P. Graves, L. Shewchuk, L.P. Wang, J.E. Cottom, H.W. Qi, H.Z. Zhao, R. Totoritis, G.F. Zhang, B. Schwartz, H. Li, S. Sweitzer, D.A. Holt, G.J. Gatto, L.S. Kallander, Identification of Purines and 7-Deazapurines as Potent and Selective Type I Inhibitors of Troponin I-Interacting Kinase (TNNI3K), Journal of Medicinal Chemistry, 58 (2015) 7431-7448.

[25] B.G. Lawhorn, J. Philp, A.P. Graves, L. Shewchuk, D.A. Holt, G.J. Gatto, L.S. Kallander, GSK114: A selective inhibitor for elucidating the biological role of TNNI3K, Bioorganic & Medicinal Chemistry Letters, 26 (2016) 3355-3358.

[26] B.G. Lawhorn, J. Philp, A.P. Graves, D.A. Holt, G.J. Gatto, L.S. Kallander, Substituent Effects on Drug-Receptor H-bond Interactions: Correlations Useful for the Design of Kinase Inhibitors, Journal of Medicinal Chemistry, 59 (2016) 10629-10641.

[27] J. Philp, B.G. Lawhorn, A.P. Graves, L. Shewchuk, K.L. Rivera, L.J. Jolivette, D.A. Holt, G.J. Gatto, L.S. Kallander, 4,6-Diaminopyrimidines as Highly Preferred Troponin I-Interacting Kinase (TNNI3K) Inhibitors, Journal of Medicinal Chemistry, 61 (2018) 3076-3088.

[28] K.G. Dave, C.J. Shishoo, M.B. Devani, R. Kalyanaraman, S. Ananthan, G.V. Ullas, V.S. Bhadti, Reaction of Nitriles Under Acidic Conditions .1. A General-Method of Synthesis of Condensed Pyrimidines, Journal of Heterocyclic Chemistry, 17 (1980) 1497-1500.

[29] Z.P. Pan, Y.J. Chen, J.Y. Liu, Q.L. Jiang, S.Y. Yang, L. Guo, G. He, Design, synthesis, and biological evaluation of polo-like kinase 1/eukaryotic elongation factor 2 kinase (PLK1/EEF2K) dual inhibitors for regulating breast cancer cells apoptosis and autophagy, European Journal of Medicinal Chemistry, 144 (2018) 517-528.

[30] F.F. Qin, Y.L. Wang, X. Jiang, Y.J. Wang, N. Zhang, X. Wen, L. Wang, Q.L. Jiang, G. He, Design, synthesis and molecular mechanisms of novel dual inhibitors of heat shock protein 90/phosphoinositide 3-kinase alpha (Hsp90/PI3K alpha) against cutaneous melanoma, Journal of Enzyme Inhibition and Medicinal Chemistry, 34 (2019) 909-926.

[31] M. Zhang, L. Jiang, J. Tao, Z.P. Pan, M.Y. He, D.Y. Su, G. He, Q.L. Jiang, Design, synthesis and biological evaluation of 4-aniline-thieno 2,3-d pyrimidine derivatives as MNK1 inhibitors against renal cell carcinoma and nasopharyngeal carcinoma, Bioorganic & Medicinal Chemistry, 27 (2019) 2268-2279.

[32] C.A. Ramos-Guzman, K. Zinovjev, I. Tunon, Modeling caspase-1 inhibition: Implications for catalytic mechanism and drug design, European Journal of Medicinal Chemistry, 169 (2019) 159-167.

[33] M. Zhu, J.B. Wang, J.W. Xie, L.P. Chen, X.Y. Wei, X. Jiang, M. Bao, Y.Y. Qiu, Q. Chen, W.L. Li, C.X. Jiang, X.O. Zhou, L.P. Jiang, P.H. Qiu, J.Z. Wu, Design, synthesis, and evaluation of chalcone analogues incorporate alpha,beta-Unsaturated ketone functionality as anti-lung cancer agents via evoking ROS to induce pyroptosis, European Journal of Medicinal Chemistry, 157 (2018) 1395-1405.

[34] B.W. Ke, M. Tian, J.J. Li, B. Liu, G. He, Targeting Programmed Cell Death Using Small-Molecule Compounds to Improve Potential Cancer Therapy, Medicinal Research Reviews, 36 (2016) 983-1035.

[35] F. Peng, N. Zhang, C.T. Wang, X.Y. Wang, W. Huang, C. Peng, G. He, B. Han, Aconitine induces cardiomyocyte damage by mitigating BNIP3-dependent mitophagy and the TNF alpha-NLRP3 signalling axis, Cell Proliferation, 53 (2020) e12701.

[36] Y.J. Wang, X. Wen, D. Hao, M.K. Zhou, X.X. Li, G. He, X. Jiang, Insights into autophagy machinery in cells related to skin diseases and strategies for therapeutic modulation, Biomedicine & Pharmacotherapy, 113 (2019) 108775.

[37] Y.J. Wang, X. Wen, N. Zhang, L. Wang, D. Hao, X. Jiang, G. He, Small-molecule compounds

target paraptosis to improve cancer therapy, Biomedicine & Pharmacotherapy, 118 (2019) 109203.

[38] H.B. He, H. Jiang, Y. Chen, J. Ye, A.L. Wang, C. Wang, Q.S. Liu, G.L. Liang, X.M. Deng, W. Jiang, R.B. Zhou, Oridonin is a covalent NLRP3 inhibitor with strong anti-inflammasome activity, Nature Communications, 9 (2018) 2550.

[39] K. Schroder, R.B. Zhou, J. Tschopp, The NLRP3 Inflammasome: A Sensor for Metabolic Danger?, Science, 327 (2010) 296-300.

[40] R.B. Zhou, A.S. Yazdi, P. Menu, J. Tschopp, A role for mitochondria in NLRP3 inflammasome activation, Nature, 469 (2011) 221-225.

[41] J.J. Ding, F. Shao, Growing a gasdermin pore in membranes of pyroptotic cells, Embo Journal, 37 (2018) e100067.

[42] J.J. Shi, Y. Zhao, K. Wang, X.Y. Shi, Y. Wang, H.W. Huang, Y.H. Zhuang, T. Cai, F.C. Wang, F. Shao, Cleavage of GSDMD by inflammatory caspases determines pyroptotic cell death, Nature, 526 (2015) 660-665.

[43] Y.P. Wang, W.Q. Gao, X.Y. Shi, J.J. Ding, W. Liu, H.B. He, K. Wang, F. Shao, Chemotherapy drugs induce pyroptosis through caspase-3 cleavage of a gasdermin, Nature, 547 (2017) 99-103.

[44] J.J. Ding, K. Wang, W. Liu, Y. She, Q. Sun, J.J. Shi, H.Z. Sun, D.C. Wang, F. Shao, Pore-forming activity and structural autoinhibition of the gasdermin family, Nature, 535 (2016) 111-116.

[45] X. Gao, X.H. Deng, X.W. Wei, H.S. Shi, H.T. Shi, T.H. Ye, B. Shao, W. Nie, Y.L. Li, M. Luo, C.Y. Gong, N. Huang, Novel thermosensitive hydrogel for preventing formation of abdominal adhesions, International Journal of Nanomedicine, 8 (2013) 2453-2463.

[46] N. Wang, C. Liu, X.X. Wang, T. He, L. Li, X.Q. Liang, L. Wang, L.J. Song, Y.Q. Wei, Q.J. Wu, C.Y. Gong, Hyaluronic Acid Oligosaccharides Improve Myocardial Function Reconstruction and Angiogenesis against Myocardial Infarction by Regulation of Macrophages, Theranostics, 9 (2019) 1980-1992.

[47] Q.J. Wu, L. Li, N. Wang, X. Gao, B.L. Wang, X.Y. Liu, Z.Y. Qian, Y.Q. Wei, C.Y. Gong, Biodegradable and thermosensitive micelles inhibit ischemia-induced postoperative peritoneal adhesion, International Journal of Nanomedicine, 9 (2014) 727-734.

[48] M. Yu, M. Zeng, Z. Pan, F. Wu, L. Guo, G. He, Discovery of novel akt1 inhibitor induces autophagy associated death in hepatocellular carcinoma cells, European journal of medicinal chemistry, 189 (2020) 112076.

[49] L. Ouyang, L. Zhang, J. Liu, L.L. Fu, D.H. Yao, Y.Q. Zhao, S.Y. Zhang, G. Wang, G. He, B. Liu, Discovery of a Small-Molecule Bromodomain-Containing Protein 4 (BRD4) Inhibitor That Induces AMP-Activated Protein Kinase-Modulated Autophagy-Associated Cell Death in Breast Cancer, Journal of Medicinal Chemistry, 60 (2017) 9990-10012.

Highlights

- 35 compounds were designed as novel TNNI3K inhibitors and discovered for their protective effects on myocardial infarction models.

- Compound 6o showed IC_{50} at sub-micromolar level both in kinase inhibitory and cellular OGD assays.

- Compound 6o alleviates pyroptosis and inflammation responses in ischemia myocardiocytes both in vitro and in vivo.

Competing interests

The authors declare no competing interests.